might attenuate vagal neurotransmission, contributing to the aggravation of disease states.

*Effects of ANG II on the transfer function from sympathetic stimulation to HR.* Although ANG II attenuated the dynamic gain of the transfer function from sympathetic stimulation to HR without affecting the natural frequency, damping ratio, or pure delay, the attenuating effect was not definitive because the effect was not significant on the steady-state response in the calculated step response (Fig. 4 and Table 4). There are conflicting reports about the effects of ANG II on sympathetic control of the heart. Starke (33) reported that ANG II (1 ng/ml) potentiated NE release in response to postganglionic sympathetic nerve stimulation in isolated rabbit hearts, whereas no effect on spontaneous or tyramine-induced NE output was observed. Farrell et al. (10) demonstrated that administration of ANG II (100 $\mu$M at 1 ml/min for 10 min; ~35–42 $\mu$g·kg$^{-1}$) into right atrial ganglionated plexus neurons via a branch of the right coronary artery caused the release of catecholamine into the myocardial interstitial fluid of anesthetized dogs, suggesting that ANG II affects intrinsic cardiac neurons. In that study, the effect of ANG II on the catecholamine release induced by cardiac sympathetic nerve stimulation was not investigated. On the other hand, Lameris et al. (19) demonstrated that administration of ANG II (0.5 ng·kg$^{-1}$·min$^{-1}$ or 30 ng·kg$^{-1}$·h$^{-1}$) into the left anterior descending coronary artery of anesthetized pigs did not yield spontaneous NE release or enhance the NE release induced by cardiac sympathetic nerve stimulation. Cardiac ganglia derived from different species can demonstrate differences in phenotype for ANG II receptors, and this may impact on the resultant neurohumoral interactions. Dendorfer et al. (7) demonstrated that ANG II (0.3 to 1 $\mu$g/kg bolus) increased renal sympathetic nerve activity during ganglionic blockade in pithed rats, suggesting direct ganglionic excitation by ANG II. In the present study, because we stimulated the postganglionic cardiac sympathetic nerve, possible direct ganglionic excitation by ANG II might not have affected the dynamic sympathetic control of HR. In addition, postganglionic CSNA did not change significantly in our experimental conditions (Tables 1 and 3), indicating that the 10 $\mu$g·kg$^{-1}$·h$^{-1}$ dose of intravenous ANG II was not high enough to produce direct ganglionic excitation.

In isolated rabbit hearts, Peach et al. (30) demonstrated that ANG II (0.2 ng/ml) inhibited NE uptake. Starke (33) reported a higher dose of ANG II (10 $\mu$g/ml) to inhibit NE uptake. In a previous study from our laboratory, blockade of neuronal NE uptake using desipramine attenuated the dynamic gain, decreased the natural frequency, and increased the pure delay of the transfer function from sympathetic stimulation to HR (28). In the present study, however, neither the natural frequency nor the pure delay was changed by ANG II, suggesting that NE uptake was not inhibited. In an in vivo study using canine hearts, Lokhandwala et al. (22) demonstrated that ANG II (100 and 200 ng·kg$^{-1}$·min$^{-1}$ or 6 and 12 $\mu$g·kg$^{-1}$·min$^{-1}$ iv) did not affect the positive chronotropic effects of either postganglionic cardiac sympathetic nerve stimulation or intravenous NE infusion. In that study, ANG II enhanced the positive chronotropic effects of sympathetic nerve stimulation but not of intravenous NE infusion after blocking neuronal NE uptake with desipramine. The authors' interpretation of the results was that ANG II facilitated NE release in response to sympathetic nerve stimulation, whereas any effects of ANG II might be masked in animals with functioning neuronal NE uptake mechanisms (22). To make matters more complex, Lameris et al. (19)

did not observe enhanced NE release during cardiac sympathetic stimulation in porcine hearts even after neuronal NE uptake was blocked with desipramine. Thus it appears that differences in species, ANG II doses, and experimental settings (in vivo vs. isolated hearts, intravenous vs. intracoronary administration, with or without the contribution of sympathetic ganglia) critically affected the experimental results. Therefore, we believe that assessing the relative effects of ANG II on the vagal and sympathetic systems is important to understand the pathophysiological roles of ANG II in the autonomic regulation of HR.

*Limitations.* Our results should be interpreted in the context of various experimental limitations. First, we obtained data from anesthetized animals. If the data had been obtained under conscious conditions, the results might have been different. Because we disabled the arterial baroreflexes and cut the autonomic efferent pathways, however, the anesthetics should not have markedly affected our results. Second, because we stimulated the postganglionic cardiac sympathetic nerve, the possible effects of ANG II on the sympathetic ganglia were not assessed. Further studies that stimulate the preganglionic cardiac sympathetic nerve with various doses of ANG II are required to determine the effects of ANG II on the cardiac sympathetic ganglionic transmission. Finally, ANG II may affect the autonomic regulation of HR chronically. Further studies focused on the effects of chronically elevated ANG II levels on the autonomic regulation of HR are required to elucidate the pathophysiological significance of elevated ANG II levels.

In conclusion, continuous intravenous administration of ANG II at a dose that did not induce direct cardiac sympathetic ganglionic excitation significantly attenuated the dynamic gain of the transfer function from vagal stimulation to HR. The attenuation of the transfer gain was observed uniformly in the frequency range under study, suggesting that ANG II can attenuate the HF component of HRV even when vagal outflow from the central nervous system remains unchanged. In addition, the same dose of ANG II did not markedly affect the dynamic gain of the transfer function from postganglionic sympathetic stimulation to HR. Although there remains a room for arguments relating to the different site of stimulation (preganglionic for vagal vs. postganglionic for sympathetic), possible disproportional suppression of the dynamic vagal and sympathetic regulation of HR likely results in a relative dominance of sympathetic control in the presence of ANG II. Because many neurohumoral elements remodel or adapt during the evolution of cardiac pathology (18), we cannot directly extrapolate the results of acute neurohumoral interactions observed in the present study to the chronic pathological situations. If we do so, however, the reduction of the HF component of HRV in patients with cardiovascular diseases, such as myocardial infarction and heart failure (34), may be partly explained by the peripheral effects of ANG II on the dynamic autonomic regulation of HR.

## APPENDIX A

*Meaning of a step response calculated from a transfer function.* We calculated a step response from a transfer function relating to the vagal or sympathetic HR control. The calculated step response is useful for time-domain interpretation of the low-pass filter characteristics described by the frequency-domain transfer function but does not necessarily conform to an experimentally estimated step response because of the following reasons. The transfer function identifies the

linear input-output relationship of a given system around a mean input signal (5 Hz for vagal and 2.5 Hz for sympathetic stimulation in the present study). The step response is then calculated for a unit change in the input signal. If we perform a kind of experiment where we change the stimulation frequency from 4.5 to 5.5 Hz for the vagal system and from 2 to 3 Hz for the sympathetic system, the resultant step response is most likely close to the calculated step response. The ordinary experimental step response is, however, estimated by a step input in which the stimulation is completely turned off before the stimulation starts. The calculated step response and the ordinary experimental step response can conform only when the system is purely linear. Whenever nonlinearities exist such as threshold and saturation commonly observed in biological systems, the two step responses disagree. Conversely, information gained by the ordinary experimental step response has a limited ability to estimate the dynamic HR response unless the system is purely linear.

Once vagal or sympathetic transfer function is identified, an impulse response of the system is obtained by an inverse Fourier transform of the transfer function. We can estimate the dynamic HR response from a convolution of a input signal and the impulse response. Figure 5 represents typical data of measured HR and calculated HR based on the transfer function. Figure 5A is a continuation of the time series obtained under the control condition depicted in Fig. 1A. Figure 5B shows a scatter plot of measured HR versus calculated HR during dynamic vagal stimulation. The solid line

indicates a linear regression line ($r^2 = 0.94$). Figure 5C is a continuation of the time series obtained under the control condition depicted in Fig. 3A. Figure 5D shows the scatter plot of measured HR versus calculated HR during dynamic sympathetic stimulation. The solid line indicates a linear regression line. Although a slight convex nonlinearity is noted between the measured HR and calculated HR, squared correlation coefficient is high ($r^2 = 0.89$). These results indicate that the transfer function can represent the dynamic HR response reasonably well.

## APPENDIX B

*Binary white noise versus Gaussian white noise.* In a previous study from our laboratory (29), we reported a corner frequency of ~0.1 Hz for a transfer function from vagal stimulation to HR, which was distinctly different from the result of the present study. Possible explanation for the discrepancy is the difference in the input variance (or power) of vagal stimulation. In the previous study, we used a Gaussian white noise (GWN) with a mean stimulation frequency of 5 Hz and a SD of 2 Hz so that the input signal covered at most 98.8% (means ± 2.5 SD) of the Gaussian distribution when the actual stimulation frequency was limited between 0 and 10 Hz. The variance of the GWN signal is 4 Hz². In contrast, the 0–10 Hz binary white noise used in the present study has a variance of 25 Hz². Hence, the binary white noise has a merit of increasing the input variance over the GWN when the stimulation frequency is limited between 0 and 10 Hz. Increasing the
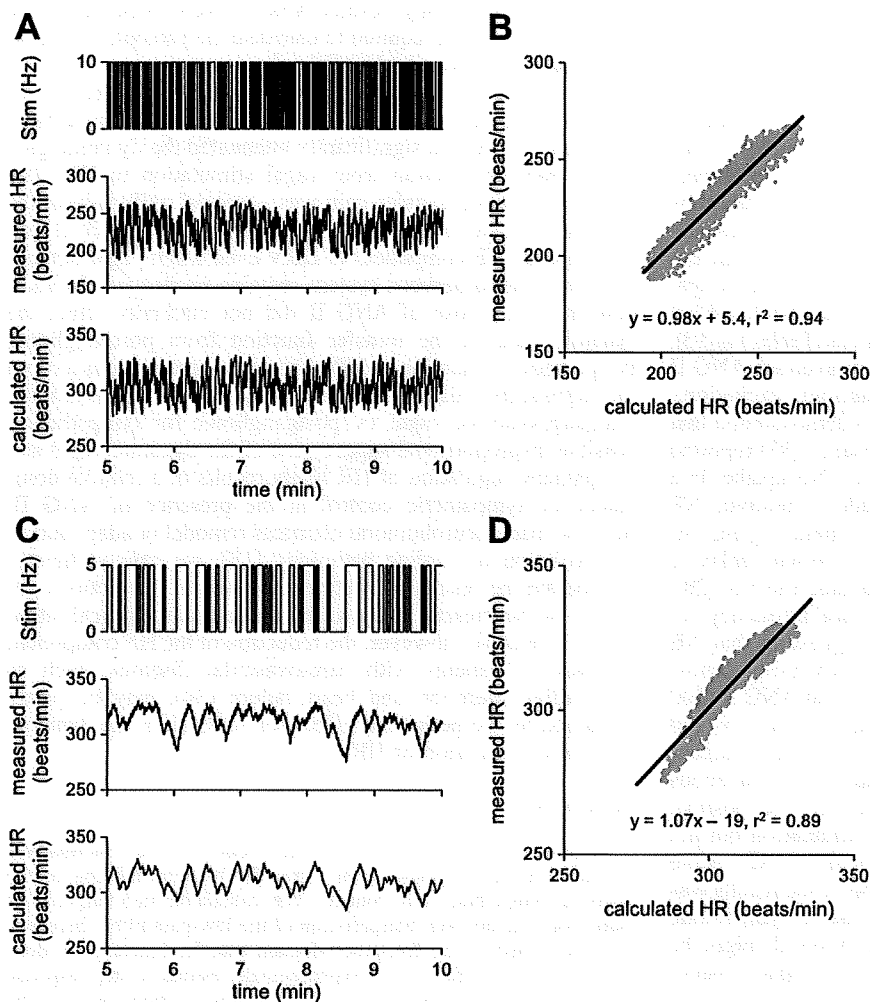


Fig. 5. A: data showing vagal stimulation (Stim), measured HR, and calculated HR based on the identified vagal transfer function of this animal. Time axis indicates the minutes after the initiation of random vagal stimulation (continuation of Fig. 1A). B: scatter plot between measured and calculated HR values. A solid line indicates a liner regression line. C: data showing sympathetic stimulation (Stim), measured HR, and calculated HR based on the identified sympathetic transfer function of this animal. Time axis indicates the minutes after the initiation of random sympathetic stimulation (continuation of Fig. 3A). D: scatter plot between measured and calculated HR values. A solid line indicates a linear regression line.

input variance is effective to increase the signal-to-noise ratio in the output signal and to improve the estimation of the transfer function.

In an earlier study on the transfer function analysis, Berger et al. (3) demonstrated that the roll-off of the vagal transfer function was gentle (i.e., the corner frequency was high) at high mean stimulatory rates and became more abrupt (i.e., the corner frequency was lower) with lower mean stimulatory rates. Although they attributed the difference in the roll-off characteristics to the difference in mean stimulatory rates, because they set the variance of input signal at ~1/4 of the mean stimulatory rates, which of the mean stimulatory rates or the input variance contributed to the determination of corner frequency seems inconclusive. Because there was no significant difference in the corner frequency between the vagal transfer functions estimated by GWNs of $5 \pm 2$ Hz and $10 \pm 2$ Hz (means $\pm$ SD) in a previous study from our laboratory (29), we speculate that the difference in the input variance rather than the mean stimulation frequency might have caused the different values of the corner frequency between the previous and the present results. This speculation requires further verification in future.

## GRANTS

## REFERENCES

1. **Akselrod S, Gordon D, Ubel FA, Shannon DC, Berger AC, Cohen RJ.** Power spectrum analysis of heart rate fluctuation: a quantitative probe of beat-to-beat cardiovascular control. *Science* 213: 220–222, 1981.
2. **Andrews PL, Dutia MB, Harris PJ.** Angiotensin II does not inhibit vagally-induced bradycardia or gastric contractions in the anaesthetized ferret. *Br J Pharmacol* 82: 833–837, 1984.
3. **Berger RD, Saul JP, Cohen RJ.** Transfer function analysis of autonomic regulation. I. Canine atrial rate response. *Am J Physiol Heart Circ Physiol* 256: H142–H152, 1989.
4. **Brigham EO.** FFT transform applications. In: *The Fast Fourier Transform and Its Applications.* Englewood Cliffs, NJ: Prentice-Hall, 1988, p. 167–203.
5. **Brooks VL.** Chronic infusion of angiotensin II resets baroreflex control of heart rate by an arterial pressure-independent mechanism. *Hypertension* 26: 420–424, 1995.
6. **Castillo-Hernandez JR, Rubio-Gayosso I, Sada-Ovalle I, Garcia-Vazquez A, Ceballos G, Rubio R.** Intracoronary angiotensin II causes inotropic and vascular effects via different paracrine mechanisms. *Vascul Pharmacol* 41: 147–158, 2004.
7. **Dendorfer A, Thornagel A, Raasch W, Grisk O, Tempel K, Dominiak P.** Angiotensin II induces catecholamine release by direct ganglionic excitation. *Hypertension* 40: 348–354, 2002.
8. **DiBona GF.** Physiology in perspective: the wisdom of the body. Neural control of the kidney. *Am J Physiol Regul Integr Comp Physiol* 289: R633–R641, 2005.
9. **Diz DI, Averill DB.** Angiotensin II/autonomic interactions. In: *Primer on the Autonomic Nervous System*, edited by Robertson D, Biaggioni I, Burnstock G, and Low PA. San Diego: Elsevier Academic Press, 2004, p. 168–171.
10. **Farrell DM, Wei CC, Tallaj J, Ardell JL, Armour JA, Hageman GR, Bradley WE, Dell'Italia LJ.** Angiotensin II modulates catecholamine release into interstitial fluid of canine myocardium in vivo. *Am J Physiol Heart Circ Physiol* 281: H813–H822, 2001.
11. **Glantz SA.** *Primer of Biostatistics* (5th ed.). New York: McGraw-Hill, 2002.
12. **Jackson EK.** Autonomic control of the kidney. In: *Primer on the Autonomic Nervous System*, edited by Robertson D, Biaggioni I, Burnstock G, and Low PA. San Diego: Elsevier Academic Press, 2004, p. 157–161.
13. **Kashihara K, Takahashi Y, Chatani K, Kawada T, Zheng C, Li M, Sugimachi M, Sunagawa K.** Intravenous angiotensin II does not affect dynamic baroreflex characteristics of the neural or peripheral arc. *Jpn J Physiol* 53: 135–143, 2003.
14. **Kawada T, Ikeda Y, Sugimachi M, Shishido T, Kawaguchi O, Yamazaki T, Alexander J Jr, Sunagawa K.** Bidirectional augmentation of heart rate regulation by autonomic nervous system in rabbits. *Am J Physiol Heart Circ Physiol* 271: H288–H295, 1996.
15. **Kawada T, Miyamoto T, Miyoshi Y, Yamaguchi S, Tanabe Y, Kamiya A, Shishido T, Sugimachi M.** Sympathetic neural regulation of heart rate is robust against high plasma catecholamine. *J Physiol Sci* 56: 235–245, 2006.
16. **Kawada T, Uemura K, Kashihara K, Jin Y, Li M, Zheng C, Sugimachi M, Sunagawa K.** Uniformity in dynamic baroreflex regulation of left and right cardiac sympathetic nerve activities. *Am J Physiol Regul Integr Comp Physiol* 284: R1506–R1512, 2003.
17. **Kawada T, Yamazaki T, Akiyama T, Li M, Zheng C, Shishido T, Mori H, Sugimachi M.** Angiotensin II attenuates myocardial interstitial acetylcholine release in response to vagal stimulation. *Am J Physiol Heart Circ Physiol* 293: H2516–H2522, 2007.
18. **Khan MH, Sinoway LI.** Congestive heart failure. In: *Primer on the Autonomic Nervous System*, edited by Robertson D, Biaggioni I, Burnstock G, and Low PA. San Diego: Elsevier Academic Press, 2004, p. 247–248.
19. **Lameris TW, de Zeeuw S, Duncker DJ, Alberts G, Boomsma F, Verdouw PD, van den Meiracker AH.** Exogenous angiotensin II does not facilitate norepinephrine release in the heart. *Hypertension* 40: 491–497, 2002.
20. **Levy MN.** Sympathetic-parasympathetic interactions in the heart. *Circ Res* 29: 437–445, 1971.
21. **Li M, Zheng C, Sato T, Kawada T, Sugimachi M, Sunagawa K.** Vagal nerve stimulation markedly improves long-term survival after chronic heart failure in rats. *Circulation* 109: 120–124, 2004.
22. **Lokhandwala MF, Amelang E, Buckley JP.** Facilitation of cardiac sympathetic function by angiotensin II: role of presynaptic angiotensin receptors. *Eur J Pharmacol* 52: 405–409, 1978.
23. **Marmarelis PZ, Marmarelis VZ.** The white noise method in system identification. In: *Analysis of Physiological Systems.* New York: Plenum, 1978, p. 131–221.
24. **Miyamoto T, Kawada T, Takaki H, Inagaki M, Yanagiya Y, Jin Y, Sugimachi M, Sunagawa K.** High plasma norepinephrine attenuates the dynamic heart rate response to vagal stimulation. *Am J Physiol Heart Circ Physiol* 284: H2412–H2418, 2003.
25. **Miyamoto T, Kawada T, Yanagiya Y, Inagaki M, Takaki H, Sugimachi M, Sunagawa K.** Cardiac sympathetic nerve stimulation does not attenuate dynamic vagal control of heart rate via α-adrenergic mechanism. *Am J Physiol Heart Circ Physiol* 287: H860–H865, 2004.
26. **Mizuno M, Kamiya A, Kawada T, Miyamoto T, Shimizu S, Sugimachi M.** Muscarinic potassium channels augment dynamic and static heart rate responses to vagal stimulation. *Am J Physiol Heart Circ Physiol* 293: H1564–H1570, 2007.
27. **Nakahara T, Kawada T, Sugimachi M, Miyano H, Sato T, Shishido T, Yoshimura R, Miyashita H, Inagaki M, Alexander J Jr, Sunagawa K.** Accumulation of cAMP augments dynamic vagal control of heart rate. *Am J Physiol Heart Circ Physiol* 275: H562–H567, 1998.
28. **Nakahara T, Kawada T, Sugimachi M, Miyano H, Sato T, Shishido T, Yoshimura R, Miyashita H, Inagaki M, Alexander J Jr, Sunagawa K.** Neuronal uptake affects dynamic characteristics of heart rate response to sympathetic stimulation. *Am J Physiol Regul Integr Comp Physiol* 277: R140–R146, 1999.
29. **Nakahara T, Kawada T, Sugimachi M, Miyano H, Sato T, Shishido T, Yoshimura R, Miyashita H, Sunagawa K.** Cholinesterase affects dynamic transduction properties from vagal stimulation to heart rate. *Am J Physiol Regul Integr Comp Physiol* 275: R541–R547, 1998.
30. **Peach MJ, Bumpus FM, Khairallah PA.** Inhibition of norepinephrine uptake in hearts by angiotensin II and analogs. *J Pharmacol Exp Ther* 167: 291–299, 1969.
31. **Potter EK.** Angiotensin inhibits action of vagus nerve at the heart. *Br J Pharmacol* 75: 9–11, 1982.
32. **Reid IA, Chou L.** Analysis of the action of angiotensin II on the baroreflex control of heart rate in conscious rabbits. *Endocrinology* 126: 2749–2756, 1990.
33. **Starke K.** Action of angiotensin on uptake, release and metabolism of $^{14}C$-noradrenaline by isolated rabbit hearts. *Eur J Pharmacol* 14: 112–123, 1971.
34. **Task Force of the European Society of Cardiology, the North American Society of Pacing and Electrophysiology.** Heart rate variability: standards of measurement, physiological interpretation and clinical use. *Circulation* 93: 1043–1065, 1996.
35. **Zimmerman BG, Sybertz EJ, Wong PC.** Interaction between sympathetic and renin-angiotensin system. *J Hypertens* 2: 581–587, 1984.

# Servo-Controlled Hind-Limb Electrical Stimulation for Short-Term Arterial Pressure Control

Toru Kawada, MD; Shuji Shimizu, MD; Hiromi Yamamoto, MD*;
Toshiaki Shishido, MD; Atsunori Kamiya, MD; Tadayoshi Miyamoto, PhD**;
Kenji Sunagawa, MD†; Masaru Sugimachi, MD

***Background:*** Autonomic neural intervention is a promising tool for modulating the circulatory system thereby treating some cardiovascular diseases.

***Methods and Results:*** In 8 pentobarbital-anesthetized cats, it was examined whether the arterial pressure (AP) could be controlled by acupuncture-like hind-limb electrical stimulation (HES). With a 0.5-ms pulse width, HES monotonically reduced AP as the stimulus current increased from 1 to 5 mA, suggesting that the stimulus current could be a primary control variable. In contrast, the depressor effect of HES showed a nadir approximately 10 Hz in the frequency range between 1 and 100 Hz. Dynamic characteristics of the AP response to HES approximated a second-order low-pass filter with dead time (gain: $-10.2 \pm 1.6$ mmHg/mA, natural frequency: $0.040 \pm 0.004$ Hz, damping ratio $1.80 \pm 0.24$, dead time: $1.38 \pm 0.13$ s, mean $\pm$ SE). Based on these dynamic characteristics, a servo-controlled HES system was developed. When a target AP value was set at 20 mmHg below the baseline AP, the time required for the AP response to reach 90% of the target level was $38 \pm 10$ s. The steady-state error between the measured and target AP values was $1.3 \pm 0.1$ mmHg.

***Conclusions:*** Autonomic neural intervention by acupuncture-like HES might provide an additional modality to quantitatively control the circulatory system. (*Circ J* 2009; **73**: 851–859)

**Key Words:** Proportional-integral controller; Transfer function

**B**ecause abnormality in the autonomic nervous system is often associated with cardiovascular diseases, treating cardiovascular diseases by autonomic neural interventions have attracted many researchers.[1–6] Recently, autonomic neural interventions using electronic devices have again gained the focus of attention as a potential modality for treating cardiovascular diseases resistant to conventional therapeutics. To name a few, chronic vagal nerve stimulation dramatically improves the survival of chronic heart failure after myocardial infarction in rats.[7] Chronic baroreceptor activation enhances the survival of pacing-induced heart failure in dogs.[8] A recent version of a device-based treatment of hypertension in human is reported.[9] A framework of electrical neural intervention is also effective to elevate arterial pressure (AP) against hypotensive events.[10–13]

Aside from direct neural stimulation, electroacupuncture

can modify autonomic balance, thereby treating cardiovascular diseases.[14–16] Although one feature of the electroacupuncture might be its long-lasting effects, immediate cardiovascular responses to acupuncture-like stimulation are also observed in several experimental settings. For example, a 60-s manual acupuncture-like stimulation of a hind limb reduces renal or cardiac sympathetic nerve activity, causing hypotension and bradycardia in anesthetized rats.[17,18] We have shown that electrical stimulation of a hind limb using acupuncture needles immediately resets the arterial baroreflex and reduces sympathetic nerve activity in anesthetized rabbits.[19] Acupuncture-like hind-limb electrical stimulation (HES) induces immediate hypotension with changes in the relationship between cardiac and renal sympathetic nerve activities in anesthetized cats.[20]

In the present study, we hypothesized that AP could be controlled by HES. Quantification of the dynamic input–output relationship between a given stimulus and the AP response is essential for artificially controlling AP.[10–12] Accordingly, the first aim was to identify the dynamic input–output relationship between HES and the AP response. The second aim was to develop a feedback controller system that could reduce AP at a prescribed target level using HES.

## Methods

### Surgical Preparation

Animal care was provided in strict accordance with the *Guiding Principles for the Care and Use of Animals in the Field of Physiological Sciences*, approved by the Physiological Society of Japan. All protocols were approved by the Animal Subject Committee of the National Cardiovascular Center. Eight adult cats weighing from 2.3 to 4.3 kg were
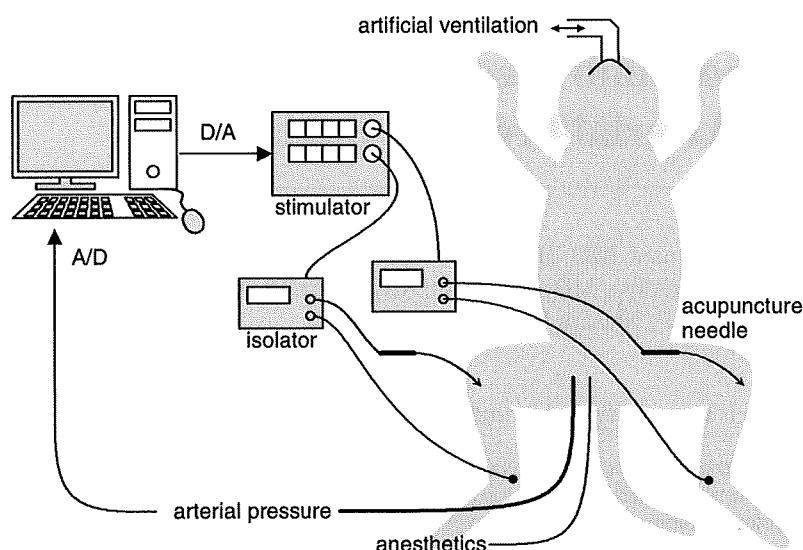
Figure 1. Experimental setup.

anesthetized by an intraperitoneal injection of pentobarbital sodium (30–35 mg/kg) and ventilated mechanically via a tracheal tube with oxygen-supplied room air. The depth of anesthesia was maintained with a continuous intravenous infusion of pentobarbital sodium (1–2 mg·kg$^{-1}$·h$^{-1}$) through a catheter inserted into the right femoral vein. Vecuronium bromide (0.5–1.0 mg·kg$^{-1}$·h$^{-1}$, iv) was given continuously to suppress muscular activity. AP was measured using a catheter-tip manometer inserted from the right femoral artery and advanced into the thoracic aorta.

## HES

In the supine position, both hind limbs were lifted to obtain a better view of the lateral sides of the lower legs. An acupuncture needle with a diameter of 0.2 mm (CE0123, Seirin-Kasei, Shimizu, Japan) was inserted into a point below the knee joint just lateral to the tibia.[20] A 23-gauge needle was inserted into the skin behind the ankle as the ground. HES was applied bilaterally via 2 independent isolators connected to an electrical stimulator (SEN 7203, Nihon Kohden, Tokyo, Japan) as shown in **Figure 1**. The pulse width was changed manually whereas the stimulus frequency and the stimulus current were controlled by a dedicated laboratory computer system. The electrical stimulation was started after the hemodynamic effects of needle insertion had disappeared, and the acupuncture needle remained inserted during each protocol.

## Protocols

**Protocol 1 (n=8)** To quantify the AP response to HES as a function of stimulus current and pulse width, we fixed the stimulus frequency at 10 Hz and changed the stimulus current stepwise from 0 to 5 mA in 1-mA increments every minute. The 6-min current test was repeated with an intervening interval of 3–5 min using different pulse widths (0.1, 0.2, 0.5 and 1 ms). The order of the pulse-width settings was randomized across the animals.

**Protocol 2 (n=8)** To quantify the AP response to HES as a function of stimulus frequency and pulse width, we fixed the stimulus current at 3 mA and changed the stimulus frequency sequentially from 0 to 100 Hz (0, 1, 2, 5, 10, 15, 20, 50 and 100 Hz). Each stimulus frequency was maintained for 1 min. The 9-min frequency test was repeated with an

intervening interval of 3–5 min using different pulse widths (0.1, 0.2, 0.5 and 1 ms). The order of the pulse-width settings was randomized across the animals.

**Protocol 3 (n=8)** To identify the dynamic input–output relationship between HES and the AP response, we randomly turned HES on and off every 2 s according to a binary white noise sequence for 30 min. The HES setting (0.5-ms pulse width, 10 Hz, 3 mA) was chosen to induce effective hypotension based on the preliminary results obtained from Protocols 1 and 2.

**Protocol 4 (n=8)** Based on the result of Protocol 3, we designed a feedback controller that could automatically adjust the stimulus frequency and the stimulus current for HES. The pulse width was fixed at 0.5 ms. To examine the performance of the feedback controller, we set a target AP value at 20 mmHg below the baseline AP and activated the feedback controller for 10 min.

The following 2 supplemental protocols were performed in 3 of the 8 cats: (1) we inserted 2 acupuncture needles into the triceps surae muscle with a distance of approximately 2.5 cm, and examined if changes in AP was associated with direct muscle stimulation (0.5-ms pulse width, 10 Hz, 3 mA). Both hind limbs were stimulated simultaneously using 2 independent isolators; and (2) we exposed the sciatic nerve after finishing Protocols 1 through 4, and examined if sectioning the sciatic nerve abolished the hemodynamic effects of HES. Unilateral HES was performed (0.5-ms pulse width, 10 Hz, 3 mA) before and after sectioning the ipsilateral sciatic nerve.

## Data Analysis

In Protocols 1 and 2, the AP value was obtained by averaging the last 10-s data at each stimulus condition. In Protocol 1, the effect of stimulus current was assessed by changes in AP from the 0-mA stimulus condition for each pulse width. In Protocol 2, the effect of stimulus frequency was assessed by changes in AP from the 0-Hz stimulus condition for each pulse width.

In Protocol 3, the transfer function from HES to AP was estimated by means of an analysis for one-input, one-output systems. Data were first resampled at 10 Hz and segmented into 8 sets of 50%-overlapping bins of 4,096 points each. For each segment, a linear trend was subtracted and a
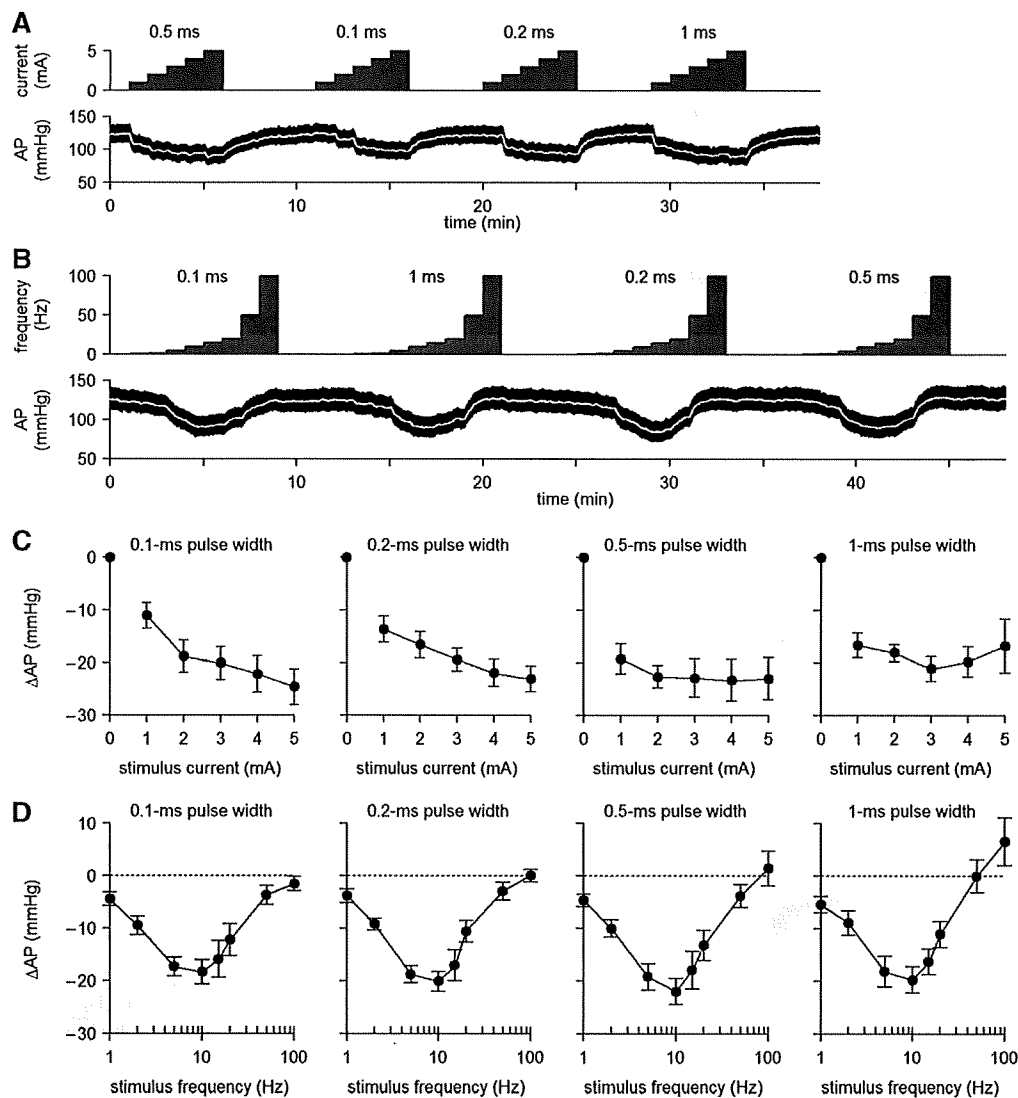
**Figure 2.** (A) Typical recordings of Protocol 1 showing the effects of stimulus current and pulse width on arterial pressure (AP). (B) Typical recordings of Protocol 2 showing the effects of stimulus frequency and pulse width on AP. The white lines in the AP traces indicate 2-s moving averaged data. (C) Changes in AP as a function of the stimulus current. AP decreased monotonously as the stimulus current increased (P<0.05). (D) Changes in AP as a function of the stimulus frequency. AP decreased more as the stimulus frequency increased from 1 to 10 Hz but the depressor effect became smaller when the stimulus frequency exceeded 10 Hz (P<0.05).

Hanning window was applied. Frequency spectra of the input and output were obtained via fast Fourier transformation. Next, the ensemble averages of input power spectral density [$S_{xx}(f)$], output power spectral density [$S_{yy}(f)$], and cross spectral density between the input and output [$S_{yx}(f)$] were calculated over the 8 segments. Finally, the transfer function from input to output [$H(f)$] was calculated as:[21]

$$H(f) = \frac{S_{yx}(f)}{S_{xx}(f)} \tag{1}$$

To quantify the linear dependence between the input and output signals in the frequency domain, a magnitude-squared coherence function [$Coh(f)$] was also calculated as:[21]

$$Coh(f) = \frac{|S_{yx}(f)|^2}{S_{xx}(f)S_{yy}(f)} \tag{2}$$

In Protocol 4, the performance of the feedback controller was evaluated by the time required for the AP response to reach 90% of the target AP decrease and by the standard deviation of the steady-state error between the target and measured AP values during the last 5 min of the 10-min feedback control. These 2 values were calculated based on the 2-s moving averaged data of AP.

**Statistical Analysis**

All data are presented as mean and SE values. In Protocol 1, changes in AP were examined by 2-way repeated-measures analysis of variance (ANOVA) using the stimulus current as one factor and the pulse width as the other factor.[22] In Protocol 2, changes in AP were examined by 2-way repeated-measures ANOVA using the stimulus frequency as one factor and the pulse width as the other factor. Differences were considered significant when P<0.05.
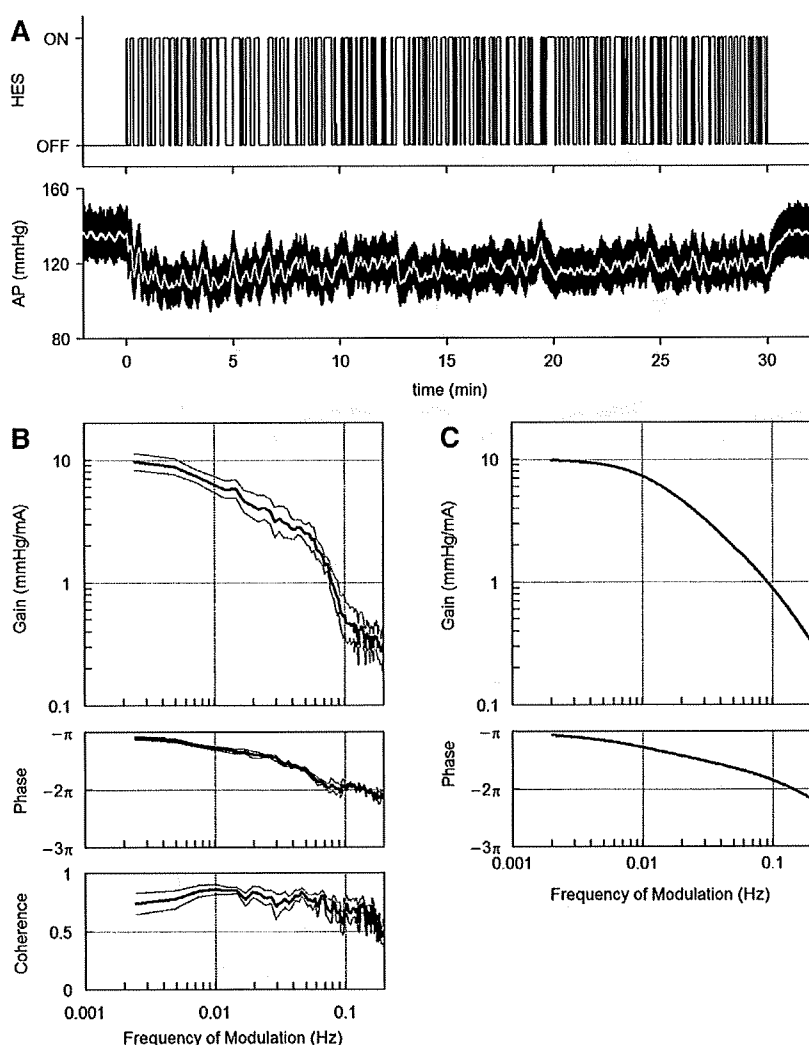
**Figure 3.** (A) Typical recordings of random hind-limb electrical stimulation (HES) and arterial pressure (AP) response. (B) Transfer function from HES to the AP response averaged from 8 cats. Thick and thin lines indicate mean and mean±SE values, respectively. (C) A model transfer function of the second-order low-pass filter with a lag time that mimics the transfer function from HES to AP.

## Results

### Relationship Between Stimulus Intensity and AP Response

Typical time series of Protocols 1 and 2 obtained from one animal are shown in **Figures 2A** and **B**, respectively. The pulse width was set in a random order. In Protocol 1, baseline AP obtained at the 0-mA stimulus condition was 118.4±5.4mmHg across the animals. Changes in mean AP as a function of stimulus current are summarized in **Figure 2C**. The decrease in AP became greater as the stimulus current increased. The overall statistical analysis indicated that the effect of the stimulus current on the magnitude of AP decrease was significant whereas that of pulse width was not. There was no significant interaction effect between the stimulus current and the pulse width.

In Protocol 2, baseline AP at the 0-Hz stimulus condition was 117.6±5.9mmHg across the animals. Changes in mean AP as a function of stimulus frequency are summarized in **Figure 2D**. The decrease in AP became greater as the stimulus frequency increased from 1 to 10Hz but it became smaller when the stimulus frequency exceeded 10Hz. At the pulse width of 1ms, the stimulus frequency of 100Hz even increased AP. The overall statistical analysis indicated

that the effect of stimulus frequency on the magnitude of AP decrease was significant whereas that of pulse width was not. There was no significant interaction effect between the stimulus frequency and the pulse width.

### Dynamic Characteristics of AP Response to HES

**Figure 3A** depicts a typical time series obtained from Protocol 3. HES was turned on and off randomly, which decreased the mean level of AP and also caused intermittent AP variations. When HES was finally turned off at 30min, AP began to increase toward the prestimulation value. A long-lasting effect of HES was not observed in the present protocol. The white line in the AP trace represents the 2-s moving averaged data of AP.

The results of transfer function analysis are depicted in **Figure 3B**. In the gain plot, the magnitude of AP response relative to the HES input was plotted in the frequency domain. The gain value became smaller as the frequency increased, indicating the low-pass characteristics of the AP response to HES. In the phase plot, AP showed an out-of-phase relationship with HES at the lowest frequency (0.0024Hz). The phase delayed more with increasing the frequency of modulation. The coherence value was approximately 0.7 in the frequency range below 0.06Hz. The
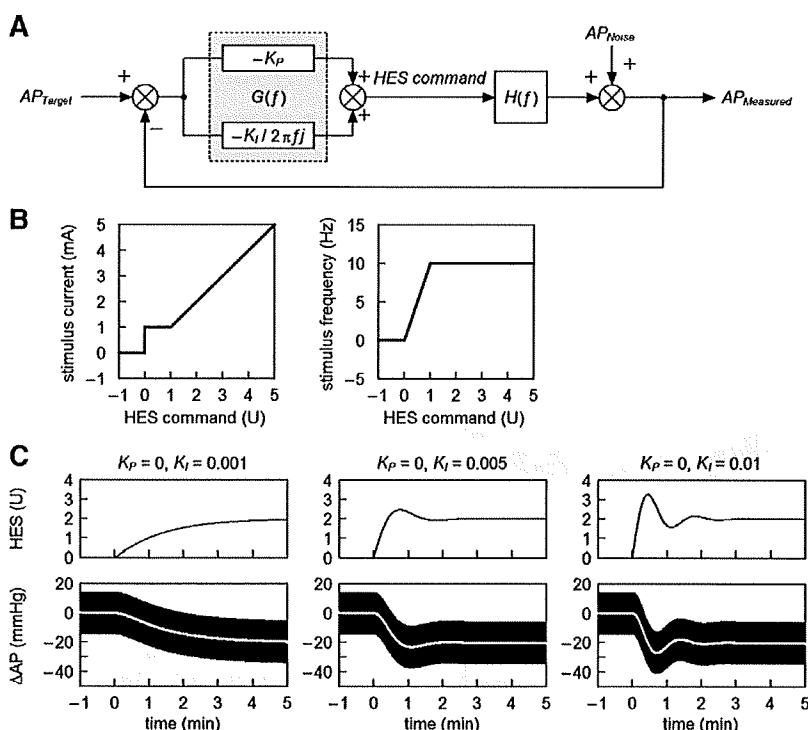
Figure 4. (A) A simplified diagram of the feedback controller utilized in the present study. $AP_{Target}$: target arterial pressure (AP); $AP_{Noise}$: noise in AP in terms of the control theory; $AP_{Measured}$: measured AP; $G(f)$: transfer function of the controller; $H(f)$: transfer function from hind-limb electrical stimulation (HES) to the AP response; $K_P$: proportional gain; $K_I$: integral gain; $f$ and $j$ denote the frequency and imaginary unit, respectively (see Appendix A for details). (B) Functions that convert the HES command into the stimulus current and the stimulus frequency. (C) Simulation results showing the feedback control of AP by HES. At time zero, the target AP was set at −20 mmHg. In the simulation, a sinusoidal wave (3 Hz, 15 mmHg in amplitude) was added to mimic the pulse pressure in AP. White lines indicate the 2-s moving averaged data of the simulated AP response.

coherence value became smaller in the frequency range above 0.1 Hz but still retained a value of 0.5, indicating that approximately half of the AP variation was explained by the HES input.

The general feature of the dynamic characteristics of the AP response to HES approximated what is known as a second order low-pass filter with a pure dead time, which is mathematically described as:

$$H(f)=\frac{-K}{1+2\zeta\frac{f}{f_N}j+\left(\frac{f}{f_N}j\right)^2}\exp(-2\pi fjL)$$

(3)

where $K$ is the steady-state gain, $f_N$ is the natural frequency, $\zeta$ is the damping ratio, and $L$ is the pure dead time. When we performed an iterative non-linear least square fitting using a downhill Simplex method, $K$, $f_N$, $\zeta$ and $L$ were estimated as 10.2±1.6 mmHg/mA, 0.040±0.004 Hz, 1.80±0.24 and 1.38± 0.13 s, respectively. A model transfer function shown in **Figure 3C** was drawn using $K$, $f_N$, $\zeta$ and $L$ of 10 mmHg/mA, 0.04 Hz, 2 and 1 s, respectively.

### Development of a Feedback Controller

We used a classical feedback controller to adjust the stimulus intensity of HES[23–25] In reference to **Figure 4A**, a HES command is determined based on a difference between measured and target AP values. $G(f)$ represents the transfer function of the controller with a proportional gain ($K_P$) and an integral gain ($K_I$). $H(f)$ indicates the model transfer function shown in **Figure 3C**. A detailed mathematical description of the controller is supplied in Appendix A.

To circumvent a threshold phenomenon in the stimulus current-AP response relationship (see Appendix B for details), the HES command (in an arbitrary unit) was transformed into the stimulus current (in mA) by a factor of 1 (**Figure 4B, Left**) only when the HES command exceeded unity. When the HES command was less than unity, the

stimulus current was held at 1 mA and the HES command was transformed into the stimulus frequency (in Hz) by a factor of 10 (**Figure 4B, Right**). The stimulation was turned off when the HES command became negative.

Several sets of simulations were conducted using the model transfer function. The target AP was set at 20 mmHg below the baseline AP. To mimic the pulse pressure in AP, a 3-Hz sinusoidal wave (corresponding to the HR of 180 beats/min) with an amplitude of 15 mmHg (corresponding to the pulse pressure of 30 mmHg) was added to the AP signal. To avoid pulsatile variation in the HES command, we set the proportional gain at zero. Under this condition, when the integral gain was set at 0.001, AP decreased gradually and it took more than 3 min to reach the target AP (**Figure 4C, Left**). When the integral gain was set at 0.005, AP decreased more promptly and reached the target AP in less than 1 min (**Figure 4C, Center**). When the integral gain was set at 0.01, the AP response occurred more rapidly but showed significant oscillations before settling (**Figure 4C, Right**). Based on these simulation results, we set the proportional gain at zero and the integral gain at 0.005 for the actual feedback-control experiment in Protocol 4.

### Performance of the Feedback Controller

**Figure 5A** demonstrates the AP regulation by HES obtained from 2 typical animals. The proportional and integral gains of the controller were not altered among the animals (ie, $K_P=0$, $K_I=0.005$). The white line in the AP trace indicates 2-s moving averaged data. The target AP was set at 20 mmHg below the AP value just before the application of HES. The feedback controller was activated for 10 min, which decreased AP at the target level. The HES command was individualized via the feedback mechanism. In the left panel of **Figure 5A**, the HES command gradually increased throughout the 10-min regulation. In the right panel of **Figure 5A**, the HES command was less than unity
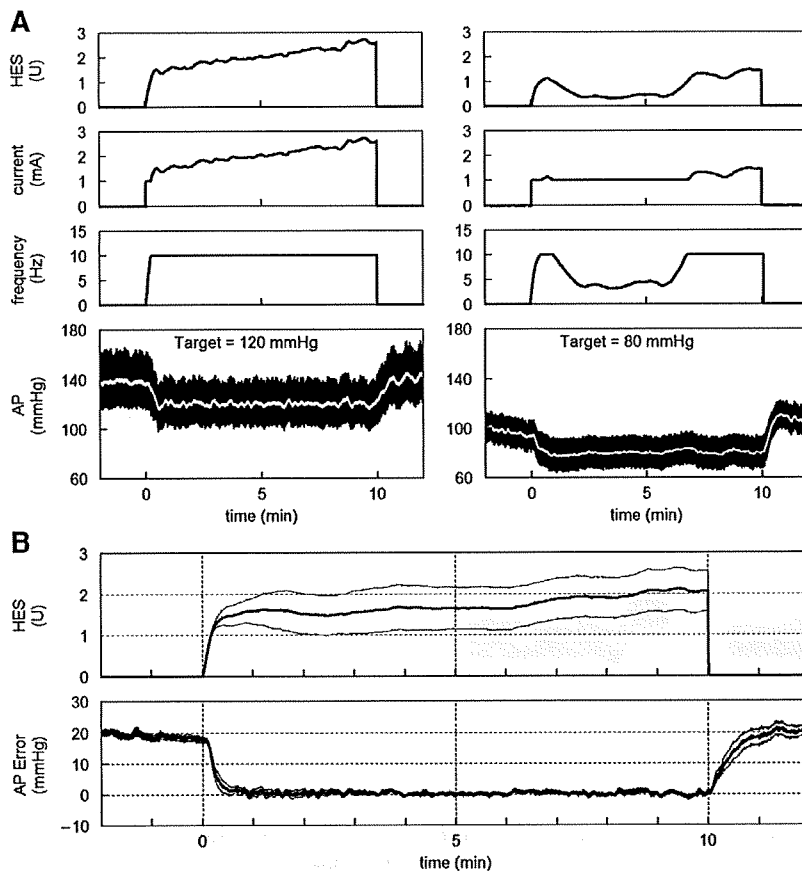
**Figure 5.** (A) Results of 10-min feedback control of arterial pressure (AP) by hind-limb electrical stimulation (HES) obtained from 2 cats. In each cat, the target AP was set at 20 mmHg below the baseline AP value. The current and frequency of HES were automatically adjusted to keep the AP at the target level. (B) HES command and the error signal between the target AP and measured AP averaged from 8 cats. The thick and thin lines indicate mean± SE values, respectively.
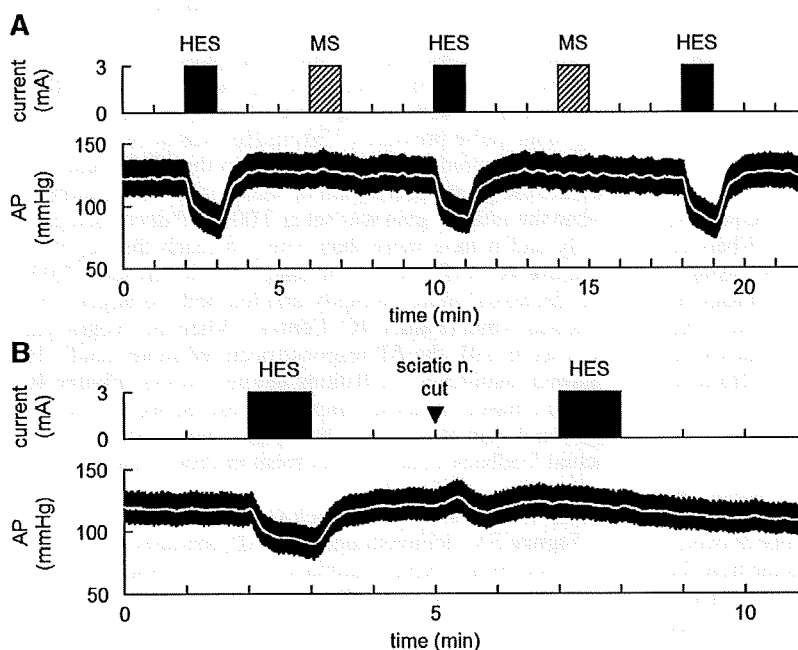


**Figure 6.** (A) Effects of electrical stimulation of the triceps surae muscle (MS) in comparison to hind-limb electrical stimulation (HES). Although muscle twitching was observed, there was no change in arterial pressure (AP) during MS. (B) Effects of sectioning the ipsilateral sciatic nerve on the HES-induced changes in AP. After the severance of the ipsilateral sciatic nerve, HES no longer produced significant hypotension.

from 1 to 7 min of the 10-min regulation. In this time period, the HES command altered the stimulus frequency rather than the stimulus current.

Mean and mean±SE values of the HES command averaged from 8 animals are shown in the top panel of **Figure**

5B. There was a large variance in the HES command among the animals, suggesting inter-individual differences in the responsiveness to HES. The target AP was 102.5±5.6 mmHg across the animals. The error signal between the target AP and measured AP disappeared in less than 1 min (**Figure 5B**,
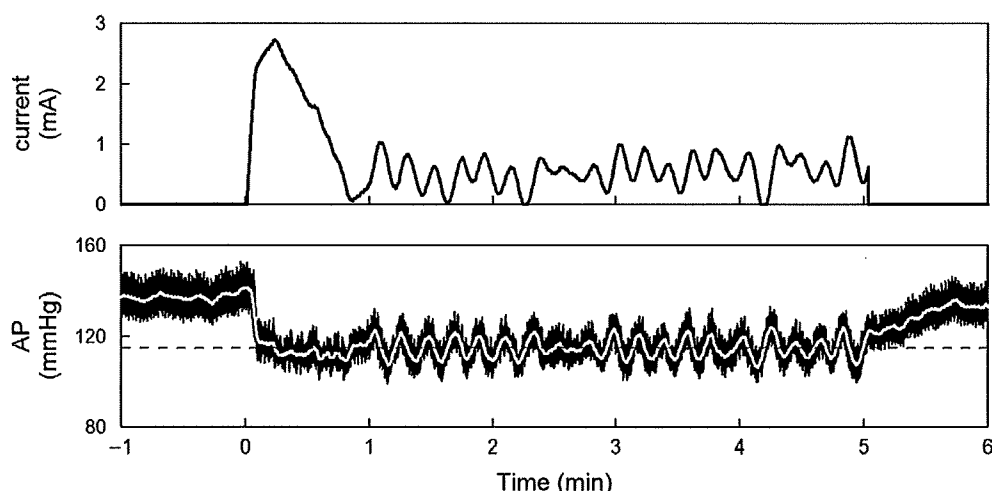
**Figure 7.** Typical recordings showing failure of controlling the intensity of the hind-limb electrical stimulation during the course of controller development. In this experimental run, only the stimulus current was controlled with a fixed stimulus frequency at 10 Hz. The controller showed on–off type controller behavior once the arterial pressure (AP) approached the target level. The horizontal dashed line indicates the target AP level.

**Bottom).** The time required for the AP response to reach 90% of the target AP decrease was 38±10s. Thereafter, the error remained very small until the end of the 10-min regulation. The standard deviation of the steady-state error was 1.3±0.1 mmHg. After the end of the feedback regulation, the error signal gradually returned to approximately 20 mmHg.

**Figure 6** represents typical results of the supplemental protocols. Electrical stimulation of the triceps surae muscle (denoted as "MS") did not change AP significantly in spite of visible twitching of the stimulated muscle, suggesting that the depressor response to HES was not the outcome of the direct muscle stimulation (**Figure 6A**). Sectioning the ipsilateral sciatic nerve abolished the depressor effect of HES, suggesting that somatic afferent signals were delivered through the sciatic nerve to the central nervous system during HES (**Figure 6B**).

## Discussion

We identified the dynamic input–output relationship between HES and the AP response. By using the model transfer function from HES to AP, we were able to develop a servo-controller that automatically adjusted the HES command to reduce AP at a prescribed target level.

### Development of the Feedback Controller

The stimulus current-AP response relationship showed a monotonous decreasing slope (**Figure 2C**). Because the effect of the pulse width was statistically insignificant, we chose the stimulus current as a primary control variable. The problem with using the stimulus current for the control variable was that a certain threshold current existed between 0 and 1 mA where the AP response to HES became discontinuous. If the stimulus current happened to be feedback controlled near the threshold current, AP showed significant oscillation around the target level (**Figure 7**, see Appendix B for details). To avoid such a problem related to the threshold current, we set the minimum current to 1 mA (above the threshold current) and used the stimulus frequency as a secondary control variable (**Figure 4B**).

The stimulus frequency-AP response relationship revealed

a valley-shaped curve with the nadir of approximately 10 Hz (**Figure 2D**). The result is similar to that obtained by stimulating hamstring muscle afferent nerves[26] From the viewpoint of controller design, the valley-shaped input–output relationship is troublesome because the proportional-integral controller only assumes a monotonous input–output relationship?[23] To avoid the problem of the valley-shaped input–output relationship, we limited the stimulus frequency to the range from 0 to 10 Hz (**Figure 4B, Right**). A similar strategy of selecting the monotonous input–output portion was used in a previous study![12]

We quantified the dynamic AP response to HES using a transfer function analysis (**Figure 3B**), and modeled it by a second-order low-pass filter with a pure dead time (**Figure 3C**). Once the transfer function is modeled, we could construct a numerical simulator for the feedback controller design (**Figure 4A**). Because the optimization of control parameters usually requires a number of trials, even if the initial values are selected via classical methods such as the Ziegler–Nichols' method?[23] it is impractical to determine optimal parameter values without using the simulator. The simulation results indicated that the integral gain value of 0.005 would provide rapid and stable AP regulation (**Figure 4C**). Because the controller was designed via intensive simulations, AP was actually controlled at the target level with a small variance (**Figure 5B, Bottom**). Note that the current and frequency of HES were automatically adjusted and individualized via the feedback mechanism (**Figure 5A**).

### Bionic Strategies Using Neural Interfaces

A framework of treating cardiovascular diseases using neural interfaces is intriguing because the autonomic nervous system exerts powerful influences on the circulatory system. In previous studies, we identified the dynamic characteristics of the arterial baroreflex system and used them to design an artificial vasomotor center. The artificial vasomotor center was able to control AP by stimulating the celiac ganglia in anesthetized rats[10,11] or the spinal cord in anesthetized cats![12] The strength and rapidity of the neural effect on the cardiovascular system compared with that of the

humoral effect[27,28] make the neural interventions desirable for the rapid and stable restoration of AP against acute disturbances such as those induced by postural changes. Gotoh et al demonstrated that a direct neural interface to the rostral ventrolateral medulla also enabled rapid and stable restoration of AP during nitroprusside-induced hypotension in conscious rats[29] The bionic system to control AP has also been applied in human subjects[13]

Although the aforementioned bionic systems aimed to maintain AP against acute hypotension by increasing sympathetic nerve activity[10–13,29] sympathoinhibition might also be required for the treatment of cardiovascular diseases accompanying sympathetic overactivity. Baroreceptor activation is one of the potential sympathoinhibitory neural modulation[8,9] In the present study we only demonstrated a framework of short-term AP control by HES. With a development of proper implanting electrodes, however, we might be able to control AP chronically using HES. Although carotid sinus baroreceptor stimulation has a potential to treat drug-resistant hypertension[9] it could activate peripheral chemoreflex by stimulating carotid bodies. HES might circumvent such unintentional chemoreflex activation. Another clinical implication will be the treatment of chronic heart failure. Although the vagal effect of HES was not evaluated in the present study, acupuncture stimulation might facilitate cardiac vagal activity[30] Because chronic intermittent vagal nerve stimulation increased the survival of chronic heart failure rats[7] chronic intermittent HES might be used as an alternative method of direct vagal nerve stimulation for the treatment of chronic heart failure.

## Study Limitations

First, we did not identify the mechanism of HES. Because sectioning of the ipsilateral sciatic nerve abolished the AP response to HES (**Figure 6B**), somatic afferent is involved in the effect of HES. In a series of studies, Chao et al and Li et al demonstrated that electroacupuncture activated group III and IV fibers in the median nerves and inhibited sympathetic outflow via activation of $\mu$- and $\delta$-opioid receptors in the rostral ventrolateral medulla[31,32] Whether a similar mechanism underlies in the rapid-onset and short-lasting effect of HES awaits further studies.

Second, we used pentobarbital anesthesia. Although peripheral neurotransmissions of norepinephrine and acetylcholine can be assessed under the same anesthesia[28,33] because pentobarbital can suppress many neurotransmitters in the central nervous system[34] anesthesia might compromise the HES effect. Further studies are required to establish the utility of HES in awake conditions.

Third, we set the proportional gain of the controller at zero to avoid pulsatile changes in the HES command. However, other approaches such as that using a low-passed signal of measured AP as a controlled variable might also be effective to avoid the pulsatile variation in the HES command.

Finally, a development of implanting electrodes is the prerequisite for chronic use of HES. Intramuscular electrodes used in functional electrical stimulation might be used for HES but further refinements are clearly needed regarding the positioning of electrodes including the depth of implantation[35,36]

In conclusion, we identified the dynamic characteristics of the AP response to acupuncture-like HES and demonstrated that a servo-controlled HES system was able to reduce AP at a prescribed target level. Although further studies are required to identify the mechanism of HES to reduce AP, acupunc-

ture-like HES would be an additional modality to exert a quantitative depressor effect on the cardiovascular system.

## References

1. Bilgutay AM, Bilgutay IM, Merkel FK, Lillehei CW. Vagal tuning: A new concept in the treatment of supraventricular arrhythmias, angina pectoris, and heart failure. *J Thorac Cardiovasc Surg* 1968; **56:** 71–82.
2. Braunwald E, Epstein SE, Glick G, Wechsler AS, Braunwald NS. Relief of angina pectoris by electrical stimulation of the carotid-sinus nerves. *N Engl J Med* 1967; **277:** 1278–1283.
3. Schwartz SI, Griffith LS, Neistadt A, Hagfors N. Chronic carotid sinus nerve stimulation in the treatment of essential hypertension. *Am J Surg* 1967; **114:** 5–15.
4. Vanoli E, De Ferrari GM, Stramba-Badiale M, Hull SS Jr, Foreman RD, Schwartz PJ. Vagal stimulation and prevention of sudden death in conscious dogs with a healed myocardial infarction. *Circ Res* 1991; **68:** 1471–1481.
5. Yang JL, Chen GY, Kuo CD. Comparison of effect of 5 recumbent positions on autonomic nervous modulation in patients with coronary artery disease. *Circ J* 2008; **72:** 902–908.
6. Baba R, Koketsu M, Nagashima M, Inasaka H, Yoshinaga M, Yokota M. Adolescent obesity adversely affects blood pressure and resting heart rate. *Circ J* 2007; **71:** 722–726.
7. Li M, Zheng C, Sato T, Kawada T, Sugimachi M, Sunagawa K. Vagal nerve stimulation markedly improves long-term survival after chronic heart failure in rats. *Circulation* 2004; **109:** 120–124.
8. Zucker IH, Hackley JF, Cornish KG, Hiser BA, Anderson NR, Kieval R, et al. Chronic baroreceptor activation enhances survival in dogs with pacing-induced heart failure. *Hypertension* 2007; **50:** 904–910.
9. Mohaupt MG, Schmidli J, Luft FC. Management of uncontrollable hypertension with a carotid sinus stimulation device. *Hypertension* 2007; **50:** 825–828.
10. Sato T, Kawada T, Shishido T, Sugimachi M, Alexander J Jr, Sunagawa K. Novel therapeutic strategy against central baroreflex failure: A bionic baroreflex system. *Circulation* 1999; **100:** 299–304.
11. Sato T, Kawada T, Sugimachi M, Sunagawa K. Bionic technology revitalizes native baroreflex function in rats with baroreflex failure. *Circulation* 2002; **106:** 730–734.
12. Yanagiya Y, Sato T, Kawada T, Inagaki M, Tatewaki T, Zheng C, et al. Bionic epidural stimulation restores arterial pressure regulation during orthostasis. *J Appl Physiol* 2004; **97:** 984–990.
13. Yamasaki F, Ushida T, Yokoyama T, Ando M, Yamashita K, Sato T. Artificial baroreflex: Clinical application of a bionic baroreflex system. *Circulation* 2006; **113:** 634–639.
14. Li P, Pitsillides KF, Rendig SV, Pan HL, Longhurst JC. Reversal of reflex-induced myocardial ischemia by median nerve stimulation: A feline model of electroacupuncture. *Circulation* 1998; **97:** 1186–1194.
15. Longhurst JC. Electroacupuncture treatment of arrhythmias in myocardial ischemia. *Am J Physiol Heart Circ Physiol* 2007; **292:** H2032–H2034.
16. Lujan HL, Kramer VJ, DiCarlo SE. Electroacupuncture decreases the susceptibility to ventricular tachycardia in conscious rats by reducing cardiac metabolic demand. *Am J Physiol Heart Circ Physiol* 2007; **292:** H2550–H2555.
17. Ohsawa H, Okada K, Nishijo K, Sato Y. Neural mechanism of depressor responses of arterial pressure elicited by acupuncture-like stimulation to a hindlimb in anesthetized rats. *J Auton Nerv Syst* 1995; **51:** 27–35.
18. Uchida S, Shimura M, Ohsawa H, Suzuki A. Neural mechanism of bradycardiac responses elicited by acupuncture-like stimulation to a hind limb in anesthetized rats. *J Physiol Sci* 2007; **57:** 377–382.
19. Michikami D, Kamiya A, Kawada T, Inagaki M, Shishido T, Yamamoto K, et al. Short-term electroacupuncture at Zusanli resets the arterial baroreflex neural arc toward lower sympathetic nerve

activity. *Am J Physiol Heart Circ Physiol* 2006; **291:** H318–H326.

20. Yamamoto H, Kawada T, Kamiya A, Kita T, Sugimachi M. Electroacupuncture changes the relationship between cardiac and renal sympathetic nerve activities in anesthetized cats. *Auton Neurosci: Basic and Clinical* 2008; **144:** 43–49.

21. Marmarelis PZ, Marmarelis VZ. Analysis of Physiological Systems. The white noise method in system identification. New York: Plenum; 1978.

22. Snedecor GW, Cochran WG. Statistical Methods, 8th ed. Ames, Iowa: University Press; 1989.

23. Åström K, Hägglund T. PID Controllers: Theory, Design, and Tuning, 2nd ed. City of Publication: Instrument Society of America; 1995.

24. Kawada T, Sunagawa G, Takaki H, Shishido T, Miyano H, Miyashita H, et al. Development of a servo-controller of heart rate using a treadmill. *Jpn Circ J* 1999; **63:** 945–950.

25. Kawada T, Ikeda Y, Takaki H, Sugimachi M, Kawaguchi O, Shishido T, et al. Development of a servo-controller of heart rate using a cycle ergometer. *Heart Vessels* 1999; **14:** 177–184.

26. Johansson B. Circulatory responses to stimulation of somatic afferents with special reference to depressor effects from muscle nerves. *Acta Physiol Scand* 1962; **Suppl 198:** 1–91.

27. Kawada T, Miyamoto T, Miyoshi Y, Yamaguchi S, Tanabe Y, Kamiya A, et al. Sympathetic neural regulation of heart rate is robust against high plasma catecholamines. *J Physiol Sci* 2006; **56:** 235–245.

28. Kawada T, Yamazaki T, Akiyama T, Shishido T, Miyano H, Sato T, et al. Interstitial norepinephrine level by cardiac microdialysis correlates with ventricular contractility. *Am J Physiol Heart Circ Physiol* 1997; **273:** H1107–H1112.

29. Gotoh TM, Tanaka K, Morita H. Controlling arterial blood pressure using a computer-brain interface. *Neuroreport* 2005; **16:** 343–347.

30. Nishijo K, Mori H, Yosikawa K, Yazawa K. Decreased heart rate by acupuncture stimulation in humans via facilitation of cardiac vagal activity and suppression of cardiac sympathetic nerve. *Neurosci Lett* 1997; **227:** 165–168.

31. Chao DM, Shen LL, Tjen-A-Looi S, Pitsillides KF, Li P, Longhurst JC. Naloxone reverses inhibitory effect of electroacupuncture on sympathetic cardiovascular reflex responses. *Am J Physiol Heart Circ Physiol* 1999; **276:** H2127–H2134.

32. Li P, Tjen-A-Looi SC, Longhurst JC. Rostral ventrolateral medullary opioid receptor subtypes in the inhibitory effect of electroacupuncture on reflex autonomic response in cats. *Auton Neurosci: Basic and Clinical* 2001; **89:** 38–47.

33. Kawada T, Yamazaki T, Akiyama T, Li M, Ariumi H, Mori H, et al. Vagal stimulation suppresses ischemia-induced myocardial interstitial norepinephrine release. *Life Sci* 2006; **78:** 882–887.

34. Adachi YU, Yamada S, Satomoto M, Watanabe K, Higuchi H, Kazama T. et al. Pentobarbital inhibits L-DOPA-induced dopamine increases in the rat striatum: An in vivo microdialysis study. *Brain Res Bull* 2006; **69:** 593–596.

35. Guevremont L, Norton JA, Mushahwar VK. Physiologically based controller for generating overground locomotion using functional electrical stimulation. *J Neurophysiol* 2007; **97:** 2499–2510.

36. Hardin E, Kobetic R, Murray L, Corado-Ahmed M, Pinault G, Sakai J,

et al. Walking after incomplete spinal cord injury using an implanted FES system: A case report. *J Rehabil Res Dev* 2007; **44:** 333–346.

## Appendix A

Framework of the Feedback Controller

**Figure 4A** is a simplified block diagram of the feedback controller system used in the present study. The controller was based on a proportional-integral controller.[23–25] $G(f)$ represents the transfer function of the controller.

$$G(f)=-K_P+\frac{-K_I}{2\pi f j} \tag{A1}$$

where $K_P$ and $K_I$ denote proportional and integral gains, respectively. $j$ represents the imaginary unit. Negative signs for the proportional and integral gains compensate for the negative input–output relationship between HES and the AP response. $H(f)$ represents a model transfer function from HES to AP determined from Protocol 3. The measured AP can be expressed as:

$$AP_{Measured}(f)=H(f)HES(f)+AP_{Noise}(f) \tag{A2}$$

where $AP_{Noise}(f)$ is the AP fluctuation such as that associated with changes in animal conditions. The controller compares the measured AP with the target AP, and adjusts the HES command to minimize the difference between them according to the following equation:

$$HES(f)=G(f)[AP_{Target}(f)-AP_{Measured}(f)] \tag{A3}$$

By eliminating $HES(f)$ from the equations A2 and A3, the overall controller characteristics are described as:

$$AP_{Measured}(f)=\frac{G(f)H(f)}{1+G(f)H(f)}AP_{Target}(f)+\frac{1}{1+G(f)H(f)}AP_{Noise}(f) \tag{A4}$$

The equation A4 indicates that if $G(f)$ is properly selected so that $G(f)H(f)$ becomes by far greater than unity, the measured AP approaches the target AP whereas the noise term is significantly attenuated over the frequency range of interest.

## Appendix B

Problem with the Threshold Current

We tried to adjust the intensity of HES by the stimulus current alone. When the stimulus current happened to be feedback controlled near a threshold current, however, the controller showed an on–off type controller behavior around the target AP level, as shown in **Figure 7**. At time zero, the controller was activated. The stimulus current increased to approximately 2.7 mA in the beginning and then decreased to a value below 1 mA, accompanying the AP reduction around a target level (a horizontal dashed line). However, the stimulus current and AP did not stabilize. Because the AP response was discontinuous at the threshold current (ie, the depressor effect of HES was abruptly turned on and off), the controller could not adjust the stimulus current in a continuous manner. To avoid this kind of on–off type controller behavior, we introduced the stimulus frequency as the secondary control variable (**Figure 4B**).

# High levels of circulating angiotensin II shift the open-loop baroreflex control of splanchnic sympathetic nerve activity, heart rate and arterial pressure in anesthetized rats

Toru Kawada · Atsunori Kamiya · Meihua Li ·
Shuji Shimizu · Kazunori Uemura · Hiromi Yamamoto ·
Masaru Sugimachi

**Abstract** Although an acute arterial pressure (AP) elevation induced by intravenous angiotensin II (ANG II) does not inhibit sympathetic nerve activity (SNA) compared to an equivalent AP elevation induced by phenylephrine, there are conflicting reports as to how circulating ANG II affects the baroreflex control of SNA. Because most studies have estimated the baroreflex function under closed-loop conditions, differences in the rate of input pressure change and the magnitude of pulsatility may have biased the estimation results. We examined the effects of intravenous ANG II ($10~\mu g~kg^{-1}~h^{-1}$) on the open-loop system characteristics of the carotid sinus baroreflex in anesthetized and vagotomized rats. Carotid sinus pressure (CSP) was raised from 60 to 180 mmHg in increments of 20 mmHg every minute, and steady-state responses in systemic AP, splanchnic SNA and heart rate (HR) were analyzed using a four-parameter logistic function. ANG II significantly increased the minimum values of AP ($67.6 \pm 4.6$ vs. $101.4 \pm 10.9$ mmHg, $P < 0.01$), SNA ($33.3 \pm 5.4$ vs. $56.5 \pm 11.5\%$, $P < 0.05$) and HR ($391.1 \pm 13.7$ vs. $417.4 \pm 11.5$ beats/min, $P < 0.01$). ANG II, however, did not attenuate the response range for AP ($56.2 \pm 7.2$ vs. $49.7 \pm 6.2$ mmHg), SNA ($69.6 \pm 5.7$ vs. $78.9 \pm 9.1\%$) or HR ($41.7 \pm 5.1$ vs. $51.2 \pm 3.8$ beats/min). The maximum gain was not affected for AP ($1.57 \pm 0.28$ vs. $1.20 \pm 0.25$), SNA ($1.94 \pm 0.34$ vs. $2.04 \pm 0.42\%$/mmHg) or HR ($1.11 \pm 0.12$ vs. $1.28 \pm 0.19$ beats $min^{-1}~mmHg^{-1}$). It is concluded that high levels of circulating ANG II did not attenuate the response range of open-loop carotid sinus baroreflex control for AP, SNA or HR in anesthetized and vagotomized rats.

**Keywords** Systems analysis · Open-loop gain · Equilibrium diagram · Carotid sinus baroreflex · Rats

## Introduction

The arterial baroreflex is an important negative feedback system that stabilizes systemic arterial pressure (AP) during daily activities. The sympathetic arterial baroreflex can be divided into the neural and peripheral arc subsystems [1]. The neural arc characterizes the input–output relation between the baroreceptor pressure input and efferent sympathetic nerve activity (SNA), whereas the peripheral arc defines the input–output relation between SNA and AP. These subsystems operate as a controller and a plant, respectively, in the negative feedback loop. Although the input signal to the neural arc is primarily the absolute input pressure level, the rate of input pressure change [1–3] and the magnitude of pulsatility [4–7] are also important input signals that critically affect the baroreflex function. Many investigators employ pharmacologic interventions, such as intravenous phenylephrine and nitroprusside administration, to estimate baroreflex function under closed-loop conditions. The rate of input pressure change and the

T. Kawada (✉) · A. Kamiya · M. Li · S. Shimizu ·
K. Uemura · M. Sugimachi
Department of Cardiovascular Dynamics,
Advanced Medical Engineering Center, National Cardiovascular
Center Research Institute, 5-7-1 Fujishirodai, Suita,
Osaka 565-8565, Japan
e-mail: torukawa@res.ncvc.go.jp

M. Li · S. Shimizu
Japan Association for the Advancement of Medical Equipment,
Tokyo 113-0033, Japan

H. Yamamoto
Division of Cardiology, Department of Internal Medicine,
Kinki University School of Medicine, Osaka 589-8511, Japan

magnitude of pulsatility, however, may vary within and between studies, which could bias the estimation results. In addition, experiments performed under baroreflex closed-loop conditions do not usually permit an evaluation of the baroreflex control of AP, because measured AP cannot be separated into signals for the input pressure and output pressure. An open-loop experiment with isolated barore-ceptor regions is therefore required to evaluate the baro-reflex function precisely.

Angiotensin II (ANG II) can affect the arterial barore-flex by centrally increasing sympathetic outflow, stimu-lating sympathetic ganglia and the adrenal medulla, and facilitating neurotransmission at sympathetic nerve endings [8]. Although an acute AP elevation induced by intrave-nous ANG II does not inhibit SNA compared to an equivalent AP elevation induced by phenylephrine, how circulating ANG II affects the baroreflex control of SNA varies among reports, i.e., intravenous ANG has been shown to attenuate [9, 10] or not attenuate [11, 12] the baroreflex control of SNA. Because it is related to the pathologic sympathoexcitation observed in such cardio-vascular diseases as chronic heart failure [13], analyzing the effects of circulating ANG II on the baroreflex open-loop system characteristics will deepen our understanding of the pathologic roles of ANG II. In the present study, we examined the effects of intravenous ANG II ($10 \ \mu g \ kg^{-1} \ h^{-1}$ or $167 \ ng \ kg^{-1} \ min^{-1}$) on the open-loop system characteristics of the baroreflex neural and periph-eral arcs in anesthetized rats. We hypothesized that ANG II would increase the minimum SNA and attenuate the range of SNA response because the maximum SNA may be saturated. Contrary to our hypothesis, ANG II increased both the minimum and maximum SNA, preserving the range of SNA response controlled by the arterial baroreflex.

## Materials and methods

Animals were cared for in strict accordance with the guiding principles for the care and use of animals in the field of physiological sciences, which has been approved by the Physiological Society of Japan. All experimental protocols were reviewed and approved by the Animal Subjects Committee at the National Cardiovascular Center.

### Baroreflex open-loop experiment

Male Sprague–Dawley rats ($n = 8$, $482 \pm 14$ g body weight, mean $\pm$ SE) were anesthetized with an intraperi-toneal injection (2 ml/kg) of a mixture of urethane (250 mg/ml) and $\alpha$-chloralose (40 mg/ml), and mechani-cally ventilated with oxygen-enriched room air. A venous catheter was inserted into the right femoral vein, and a tenfold dilution of the anesthetic mixture was administered ($2 \ ml \ kg^{-1} \ h^{-1}$) to maintain an appropriate level of anes-thesia. An arterial catheter was inserted into the right femoral artery to measure AP. A cardiotachometer was used to measure heart rate (HR). Another venous catheter was inserted into the left femoral vein to administer Ringer's solution with or without ANG II.

We exposed a postganglionic branch of the splanchnic nerve through a left flank incision and attached a pair of stainless steel wire electrodes (Bioflex wire AS633, Cooner Wire, CA) to record SNA. The nerve and electrodes were covered with silicone glue (Kwik-Sil, World Precision Instruments, Sarasota, FL) for insulation and fixation. To quantify the nerve activity, the preamplified nerve signal was band-pass filtered at 150–1,000 Hz, and then full-wave rectified and low-pass filtered with a cutoff frequency of 30 Hz. Pancuronium bromide ($0.4 \ mg \ kg^{-1} \ h^{-1}$) was administered to prevent muscular activity from contami-nating the SNA recording. At the end of the experiment, we confirmed the disappearance of SNA after an intravenous bolus injection of hexamethonium bromide (60 mg/kg) and recorded the noise level.

The vagal and aortic depressor nerves were sectioned at the neck to avoid reflexes from the cardiopulmonary region and aortic arch. The bilateral carotid sinuses were isolated from the systemic circulation according to previously reported procedures [14, 15]. Briefly, a fine needle with a 7-0 polypropylene suture (PROLENE, Ethicon, GA, USA) was passed through the tissue between the external and internal carotid arteries, and the external carotid artery was ligated close to the carotid bifurcation. The internal carotid artery was embolized using two or three bearing balls (0.8 mm in diameter, Tsubaki Nakashima, Nara, Japan), which were injected from the common carotid artery. The isolated carotid sinuses were filled with warmed Ringer's solution through catheters inserted via the common carotid arteries. Carotid sinus pressure (CSP) was controlled using a servo-controlled piston pump. Heparin sodium (100 U/kg) was given intravenously to prevent blood coagulation. Body temperature was maintained at approximately 38°C with a heating pad.

### Protocols

Sympathetic nerve activity and AP responses to CSP per-turbations were monitored for at least 30 min after the surgical preparation was completed. If these responses became smaller within this period, the animal was dis-carded from the study. Possible causes for deteriorations in the responses include surgical damage to the carotid sinus nerves and brain ischemia due to bilateral carotid occlusion.

The CSP was decreased to 60 mmHg for 4–6 min, and then increased every minute from 60 to 180 mmHg using 20-mmHg increments. At least four step cycles were performed under control conditions while Ringer's solution was continuously administered (6 ml kg$^{-1}$ h$^{-1}$). After recording the control data, the intravenous Ringer's solution was replaced with that containing ANG II (167 ng kg$^{-1}$ min$^{-1}$). The dose of ANG II was chosen to induce a significant pressor effect based on previous studies [16, 17]. At least three step cycles were performed during ANG II administration.

### Data analysis

Data were sampled at 200 Hz using a 16-bit analog-to-digital converter and stored on the hard disk of a dedicated laboratory computer system. To quantify the open-loop static characteristics of the carotid sinus baroreflex, mean values of SNA, AP and HR were calculated during the last 10 s at each CSP level. The effects of ANG II were assessed during the third step cycle after ANG II administration began, at which point the hemodynamic responses to ANG II appeared to reach steady state. Comparisons were made against two control step cycles (control 1 and control 2, see Fig. 1). In each animal, the SNA noise level recorded after the administration of hexamethonium bromide was set to zero. The SNA values obtained at a CSP level of 60 mmHg during control 1 and control 2 were averaged and defined as 100%.

The open-loop characteristics of the AP, SNA and HR responses as functions of CSP were quantified by fitting a four-parameter logistic function to the obtained data as follows [18]:

$$y = \frac{P_1}{1 + \exp[P_2(\text{CSP} - P_3)]} + P_4.$$

where $y$ represents AP, SNA or HR; $P_1$ is the response range (the difference between the maximum and minimum values of $y$); $P_2$ is a slope coefficient; $P_3$ is the midpoint in CSP; $P_4$ is the minimum value of $y$. The maximum gain or maximum slope of the sigmoidal curve was obtained from $P_1P_2/4$.

The open-loop characteristics of the baroreflex peripheral arc (i.e., SNA–AP relation) were quantified using linear regression analysis as follows:

$$\text{AP} = a \times \text{SNA} + b.$$

where $a$ and $b$ represent the slope and intercept of the regression line, respectively.

### Statistical analysis

All parameters were compared among control 1, control 2 and ANG II conditions using repeated-measures analysis of variance [19]. When there was a significant difference among the three conditions, all pairwise comparisons were performed using the Student-Neuman-Keuls test. Differences were considered significant at $P < 0.05$. All data are expressed as mean and SE values.

### Results

Typical experimental recordings are shown in Fig. 1. The stepwise input from 60 to 180 mmHg was imposed repeatedly on CSP. An increase in CSP decreased SNA. m-SNA represents the 5-s moving-average signal of the percentage of SNA. AP and HR were also decreased in response to increases in CSP. After ANG II administration was initiated, the levels of SNA, AP and HR all increased compared to the levels before ANG II administration. The responses in SNA, AP and HR to the CSP input appeared to be preserved. Data obtained from the three boxes with dashed lines (control 1, control 2 and ANG II) were used for the statistical analysis.

The open-loop characteristics of the total baroreflex revealed sigmoidal nonlinearity (Fig. 2a). No significant differences were observed between the two control conditions. ANG II significantly increased the minimum AP without affecting the response range, slope coefficient or midpoint in CSP (Table 1). The maximum gain of the total baroreflex was unchanged. The open-loop characteristics of the baroreflex control of HR also approximated sigmoidal nonlinearity (Fig. 2b), and no significant differences were observed between the two control conditions. ANG II significantly increased the minimum HR without affecting the response range, slope coefficient or midpoint in CSP (Table 1). The maximum slope of the baroreflex control of HR was unchanged.

The total baroreflex was decomposed into the neural and peripheral arc subsystems. The open-loop characteristics of the baroreflex neural arc revealed sigmoidal nonlinearity (Fig. 3a). There were no significant differences between the two control conditions. ANG II significantly increased the minimum SNA (Table 1). Although the midpoint in CSP was lower in ANG II than in control 1, the difference was not significant when compared with control 2. ANG II did not affect the response range, slope coefficient or the maximum slope of the baroreflex control of SNA. The open-loop characteristics of the baroreflex peripheral arc approximated a straight line (Fig. 3b). There were no significant differences between the two control conditions. ANG II significantly increased the intercept of the regression line (Table 1). AP at 100% SNA did not change significantly, suggesting that the slope of the regression line could be shallower under the ANG II condition. The slope of the
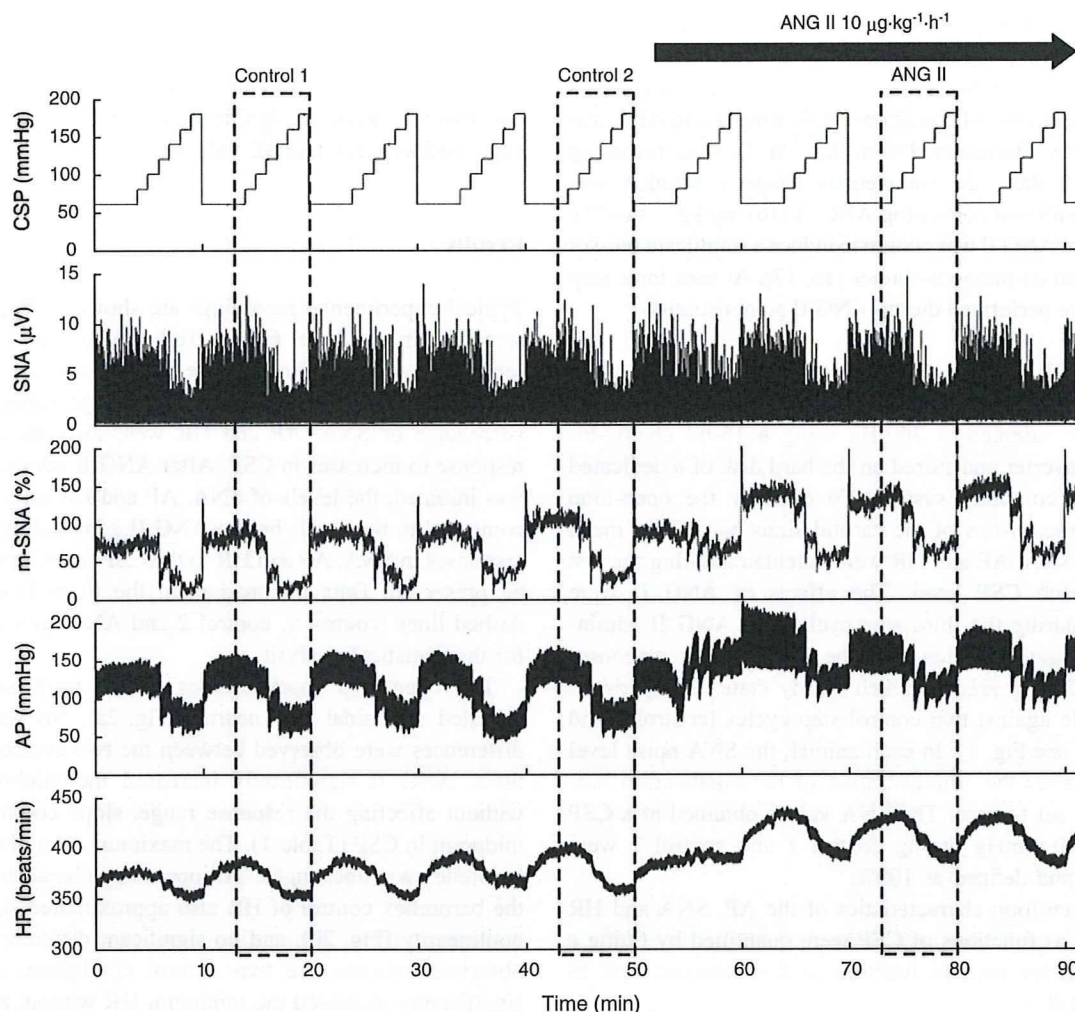
**Fig. 1** Typical recordings of carotid sinus pressure (*CSP*), splanchnic sympathetic nerve activity (*SNA*), the 5-s moving-average signal of the percentage of SNA (*m-SNA*), systemic arterial pressure (*AP*) and heart rate (*HR*). CSP was changed stepwise from 60 to 180 mmHg in 20-mmHg increments every minute. Angiotensin II (ANG II) was administered intravenously while the CSP perturbation was continued. ANG II significantly increased SNA, AP and HR. Reflex responses in SNA, AP and HR were not attenuated in the presence of ANG II. *Dashed boxes* indicate the step cycles used for the statistical analysis

regression line, however, was not statistically different among the three conditions.

An equilibrium diagram or a balance diagram was obtained by drawing the neural and peripheral arcs using SNA as the common abscissa and CSP or AP as an ordinate [20–22]. Figure 4 illustrates the equilibrium diagrams under the control 2 (dashed line) and ANG II (solid line) conditions, which were drawn based on the mean parameter values from the logistic function and regression line. Open and filled circles represent the closed-loop operating points under the control 2 and ANG II conditions, respectively. Although AP at the closed-loop operating point was significantly increased by the intravenous ANG II, SNA at the closed-loop operating point was unchanged (Table 1). If ANG II affected the peripheral arc alone, the closed-operating point may have been located at the point depicted by the open triangle. If ANG II affected the neural arc alone, the closed-loop operating point may have been located at the point depicted by the filled triangle.

## Discussion

### Effects of ANG II on open-loop baroreflex control of SNA

Intravenous ANG II at 167 ng kg$^{-1}$ min$^{-1}$ shifted the open-loop baroreflex control of splanchnic SNA toward higher SNA values without attenuating the size of the response range (Fig. 3a; Table 1). The maximum slope was
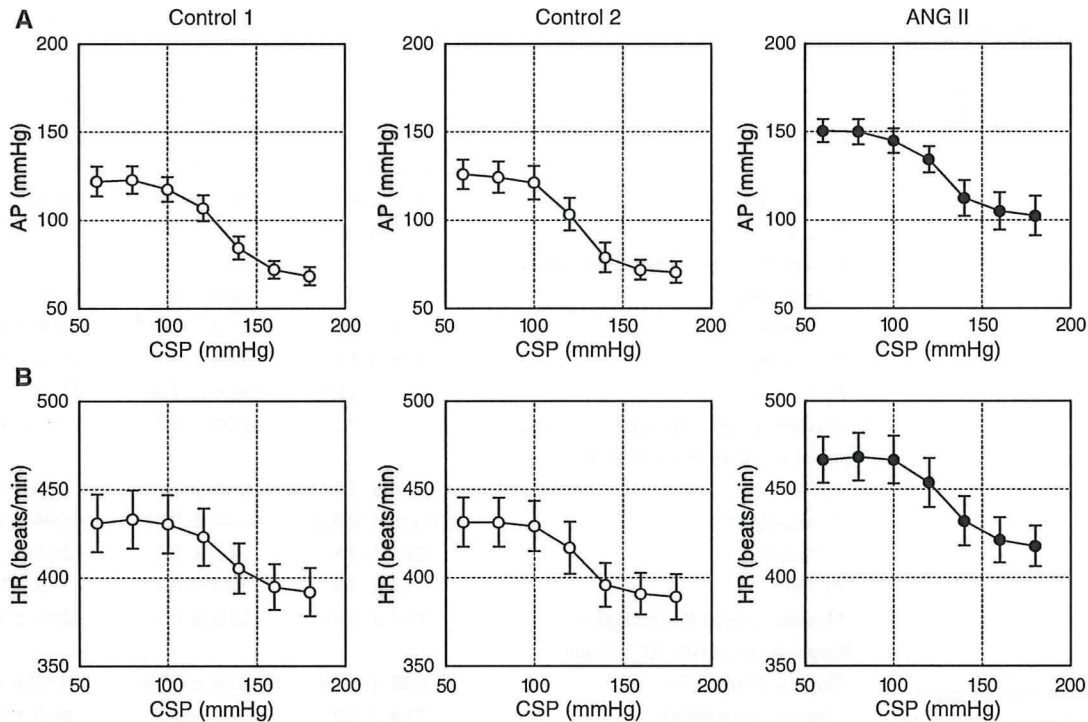
**Fig. 2** **a** Averaged input–output relation of the total baroreflex. AP decreased in response to an increase in the CSP. ANG II increased AP, while the range of the AP response was preserved. **b** Averaged input–output relation of the arterial baroreflex control of HR. HR decreased in response to an increase in the CSP. ANG II increased the HR, while the range of the HR response was preserved

unaltered, which agreed with a previous study from our laboratory in which intravenous ANG II at $100 \text{ ng kg}^{-1} \text{ min}^{-1}$ did not change the dynamic gain of the neural arc in anesthetized rabbits [23]. In contrast, Sanderford and Bishop demonstrated that ANG II at 10 or $20 \text{ ng kg}^{-1} \text{ min}^{-1}$ significantly reduced the maximum renal SNA and attenuated the range of baroreflex control of renal SNA in conscious rabbits [9, 24]. On the other hand, Tan et al. [12] demonstrated that intravenous ANG II at $400 \text{ ng kg}^{-1} \text{ min}^{-1}$ did not increase the levels of renal SNA in anesthetized rats. The regional differences in SNA may partly explain the conflicting results, because Fukiyama [25] noted that ANG II infusion (3.5–9.5 $\text{ng kg}^{-1} \text{ min}^{-1}$) through the vertebral artery resulted in an increase in splanchnic SNA, a transient increase followed by a decrease in renal SNA, and no change in cardiac SNA in anesthetized dogs.

Activation of the renin–angiotensin system contributes to the pathologic sympathoexcitation observed in such cardiovascular diseases as chronic heart failure. In addition to the augmented cardiac sympathetic reflex, impairment of the arterial baroreflex is thought to contribute to sympathoexcitation [13]. The present results indicate that ANG II may increase SNA, but it does not attenuate baroreflex control of SNA such that the magnitude of the SNA response to the input pressure change is preserved (Fig. 3a). ANG II also did not attenuate the gain of the total baroreflex estimated by the magnitude of the AP response to the input pressure change (Fig. 2a). Therefore, the observed weakening of the baroreflex reported in patients with chronic heart failure may not be readily explainable by an acute effect of high circulating levels of ANG II.

Several studies have demonstrated that ANG II-induced hypertension does not decrease SNA via the arterial baroreflex compared to equivalent hypertension induced by phenylephrine [10, 12, 26]. Although those results seem to be consistent with the idea that ANG II blunts the arterial baroreflex, the experimental protocol is confusing, and the interpretation could be wrong as follows. The intersection between the neural and peripheral arcs in the baroreflex equilibrium diagram conforms to the closed-loop operating point [21, 27, 28]. In the present study, ANG II significantly increased AP without significant changes in SNA at the closed-loop operating point (Fig. 4, open vs. filled circles; Table 1). If we calculate the baroreflex control of SNA based on ANG II-induced hypertension, therefore, we would incorrectly conclude that the baroreflex does not control SNA. If we observe the SNA response to changes in

**Table 1** Effects of intravenous angiotensin II (ANG II) on the parameters of logistic functions and regression lines of the open-loop baroreflex characteristics

| | Control 1 | Control 2 | ANG II |
|---|---|---|---|
| Total baroreflex, CSP–AP relation | | | |
| $P_1$ (mmHg) | 56.2 ± 7.2 | 56.3 ± 6.4 | 49.7 ± 6.2 |
| $P_2$ (mmHg$^{-1}$) | 0.116 ± 0.019 | 0.118 ± 0.015 | 0.094 ± 0.013 |
| $P_3$ (mmHg) | 129.2 ± 3.5 | 124.5 ± 2.8 | 125.7 ± 3.2 |
| $P_4$ (mmHg) | 67.6 ± 4.6 | 69.7 ± 5.8 | 101.4 ± 10.9**,†† |
| Maximum gain | 1.57 ± 0.28 | 1.58 ± 0.22 | 1.20 ± 0.25 |
| Baroreflex control of HR, CSP–HR relation | | | |
| $P_1$ (beats/min) | 41.7 ± 5.1 | 43.9 ± 6.2 | 51.2 ± 3.8 |
| $P_2$ (mmHg$^{-1}$) | 0.123 ± 0.027 | 0.133 ± 0.018 | 0.099 ± 0.013 |
| $P_3$ (mmHg) | 131.8 ± 3.8 | 125.8 ± 3.6 | 129.1 ± 2.6 |
| $P_4$ (beats/min) | 391.1 ± 13.7 | 388.0 ± 12.6 | 417.4 ± 11.5**,†† |
| Maximum slope (beats min$^{-1}$ mmHg$^{-1}$) | 1.11 ± 0.12 | 1.39 ± 0.23 | 1.28 ± 0.19 |
| Neural arc, CSP–SNA relation | | | |
| $P_1$ (%) | 69.6 ± 5.7 | 66.5 ± 7.4 | 78.9 ± 9.1 |
| $P_2$ (mmHg$^{-1}$) | 0.110 ± 0.016 | 0.124 ± 0.015 | 0.098 ± 0.011 |
| $P_3$ (mmHg) | 133.2 ± 3.8 | 127.3 ± 3.1 | 126.0 ± 3.4* |
| $P_4$ (%) | 33.3 ± 5.4 | 35.0 ± 6.4 | 56.5 ± 11.5*,† |
| Maximum slope (%/mmHg) | 1.94 ± 0.34 | 2.02 ± 0.33 | 2.04 ± 0.42 |
| Peripheral arc, SNA–AP relation | | | |
| Slope, $a$ (mmHg/%) | 0.85 ± 0.09 | 0.86 ± 0.06 | 0.66 ± 0.10 |
| Intercept, $b$ (mmHg) | 37.8 ± 5.2 | 36.9 ± 5.5 | 68.0 ± 10.6**,†† |
| AP at 100% SNA (mmHg) | 122.7 ± 9.9 | 122.7 ± 7.0 | 134.4 ± 4.9 |
| Operating point | | | |
| AP (mmHg) | 111.4 ± 5.0 | 110.3 ± 5.1 | 128.1 ± 4.4**,†† |
| SNA (%) | 90.6 ± 7.4 | 85.8 ± 2.1 | 94.3 ± 5.9 |

Data are mean and SE values

*CSP* Carotid sinus pressure, *AP* arterial pressure, *HR* heart rate, *SNA* sympathetic nerve activity

* $P < 0.05$ and ** $P < 0.01$ from control 1, † $P < 0.05$ and †† $P < 0.01$ from control 2

CSP, however, the baroreflex should be able to control SNA in the presence of ANG II (Fig. 3a). Lumbers et al. [29] pointed out a problem regarding the use of ANG II-induced hypertension as an input perturbation to evaluate the baroreflex.

### Effects of ANG II on the baroreflex peripheral arc

The open-loop system characteristics of the baroreflex peripheral arc, assessed using the AP response as a function of SNA, approximated a straight line under both control and ANG II-treated conditions (Fig. 3b), suggesting that the splanchnic SNA may represent changes in systemic SNA that controlled the AP. ANG II significantly increased the intercept of the regression line, reflecting its direct vasoconstrictive effect (Table 1). Because the AP at 100% SNA did not differ among the three conditions, the slope could be shallower in the presence of ANG II. In other words, ANG II appears to elevate the AP to a greater extent for the lower SNA range. Although both the modulation of sympathetic neurotransmission and direct vasoconstriction contribute to the elevation of AP, the fact that ANG II enhances the sympathetic neurotransmission more with a

lower stimulation frequency [30, 31] may, in part, account for the greater ANG II-induced increase in AP for the lower SNA range.

### Effects of ANG II on the open-loop sympathetic baroreflex control of HR

The baroreflex control of HR showed changes similar to those observed for SNA. Intravenous ANG II increased both the minimum and maximum HR while not significantly affecting the response range of HR or the maximum slope of the response (Fig. 2b; Table 1). The midpoint in CSP was not changed by ANG II. Therefore, the open-loop baroreflex control of HR shifted upward to higher HR values without a concomitant rightward shift to higher CSP values in the present study. In contrast, previous studies reported a rightward shift in the baroreflex control of HR toward higher input pressure values during acute [11, 32] and chronic [33] administration of ANG II in conscious rabbits. Reid and Chou [32] indicated that the inhibition of vagal tone to the heart played a significant role in resetting the baroreflex control of HR in conscious rabbits. It is likely that the rightward shift in the baroreflex control of
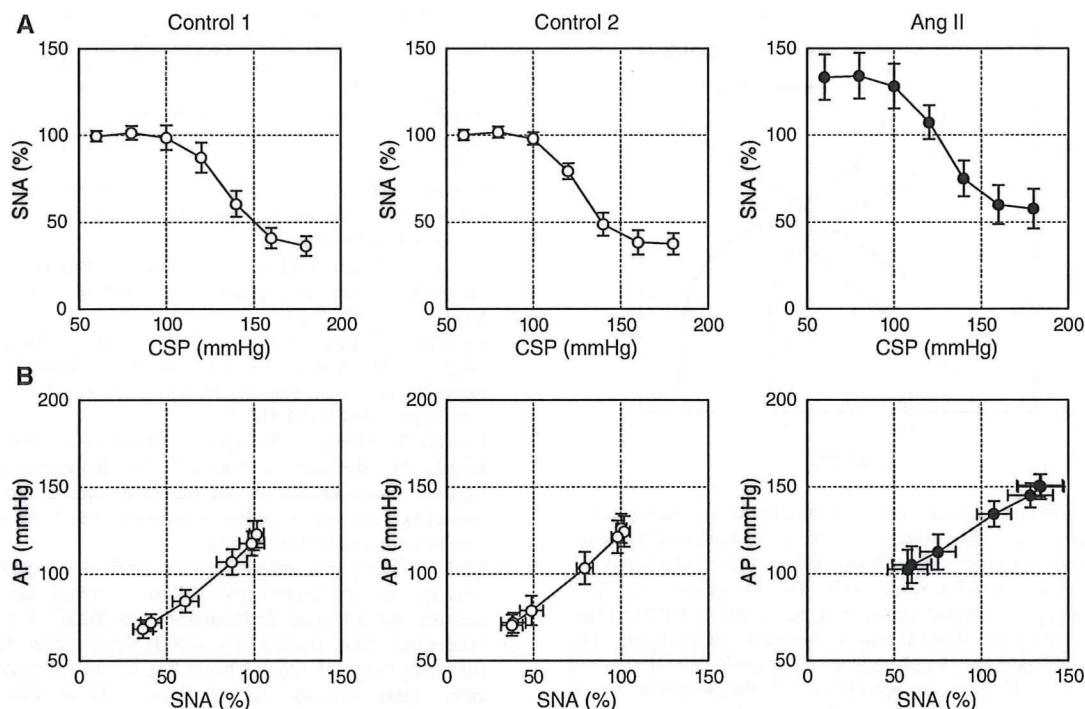
**Fig. 3** **a** Averaged input–output relation of the baroreflex neural arc or the arterial baroreflex control of SNA. SNA decreased in response to an increase in the CSP. ANG II increased SNA, while the range of the SNA response was preserved. **b** Averaged input–output relation of the baroreflex peripheral arc. AP increased in response to an increase in SNA. ANG II increased the AP, an effect that was greater for lower SNA

HR by ANG II was not observed in the present study because the vagal nerves were sectioned.

Limitations

First, we performed the experiments in anesthetized animals, and comparisons with results obtained in conscious animals should be made carefully. Circulating levels of ANG II may vary under anesthesia, which could have affected the present results. For instance, reported plasma ANG II concentration in pithed rats is approximately 400 pg/ml [16], which exceeds the plasma ANG II concentration reported in rats with heart failure [34]. Second, although the dose of ANG II used in the present study was within or below those used in previous studies in rats [12, 16, 17], Brown et al. demonstrated that intravenous ANG II at 20 and 270 ng $kg^{-1}$ $min^{-1}$ increased the plasma ANG II concentration from approximately 80 pg/ml to 140 and 2,000 pg/ml, respectively [35]. Based on those data, the plasma ANG II concentration might have been increased beyond a physiologically relevant range to approximately 1,200 pg/ml in the present study. Therefore, the observed effect of ANG II on the arterial baroreflex should be interpreted as pharmacologic. Effects of circulating ANG II

can be different when examined in different doses. Third, there was large variation in HR values among the animals (Fig. 2b). Increasing the number of animals would reduce this variation. Nevertheless, data from the eight rats was sufficient to perform statistical analyses and draw reasonable conclusions. Fourth, we occluded the common carotid arteries to isolate the carotid sinuses. Although the vertebral arteries were kept intact and the effects of ANG II were examined using the same preparation, the possibility cannot be ruled out that the carotid occlusion affected the present results. Finally, we cut the vagal nerves to obtain the open-loop condition for the carotid sinus baroreflex. Further studies are needed to clarify the effects of ANG II on the baroreflex control of the cardiovascular system through the vagal system.

**Conclusion**

The present study indicates that high circulating levels of ANG II significantly increased splanchnic SNA but did not acutely attenuate the range of arterial baroreflex control of SNA. The ranges of the total baroreflex response and the baroreflex control of HR were also preserved during ANG
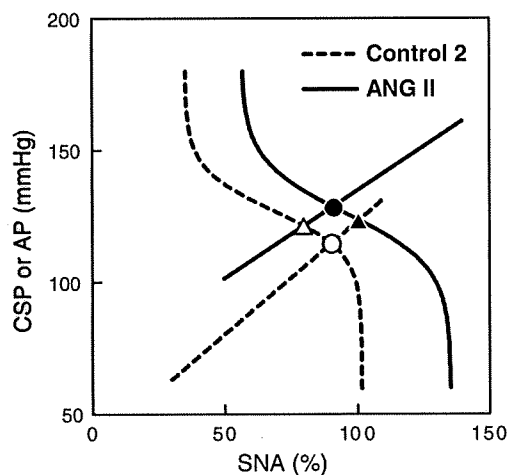
**Fig. 4** Equilibrium diagrams between the arterial baroreflex neural and peripheral arcs. The *dashed* and *solid curves* represent the open-loop characteristics of the baroreflex neural arc under the control and ANG II-treated conditions, respectively. The *dashed* and *solid lines* represent the open-loop characteristics of the baroreflex peripheral arc under the control and ANG II-treated conditions, respectively. The *open circle* indicates the closed-loop operating point under the control condition. ANG II causes an upward shift in the peripheral arc. If ANG II does not affect the neural arc, the closed-loop operating point would be at the point depicted by the *open triangle*. In this case, the estimation of baroreflex control of SNA based on the closed-loop operating points (the *open circle* and *open triangle*) approximates the slope of the baroreflex neural arc (*dashed curve*). ANG II, however, causes a rightward shift in the neural arc. Thus, the estimation of the baroreflex control of SNA based on closed-loop operating points (the *open* and *filled circles*) does not match the slope of the neural arc under either the control (*dashed curve*) or ANG II-treated condition (*solid curve*)

II administration. ANG II does modify the arterial baroreflex in that it increases SNA at a given baroreceptor pressure level but does not appear to attenuate the range of arterial baroreflex control of SNA, HR or AP.

## References

1. Ikeda Y, Kawada T, Sugimachi M, Kawaguchi O, Shishido T, Sato T, Miyano H, Matsuura W, Alexander J Jr, Sunagawa K (1996) Neural arc of baroreflex optimizes dynamic pressure regulation in achieving both stability and quickness. Am J Physiol 271:H882–H890
2. Kawada T, Yamamoto K, Kamiya A, Ariumi H, Michikami D, Shishido T, Sunagawa K, Sugimachi M (2005) Dynamic

3. Sato T, Kawada T, Shishido T, Miyano H, Inagaki M, Miyashita H, Sugimachi M, Kneupfer MM, Sunagawa K (1998) Dynamic transduction properties of in situ baroreceptors of rabbit aortic depressor nerve. Am J Physiol Heart Circ Physiol 274:H358–H365
4. Chapleau MW, Abboud FM (1987) Contrasting effects of static and pulsatile pressure on carotid baroreceptor activity in dogs. Circ Res 61:648–658
5. Kawada T, Fujiki N, Hosomi H (1992) Systems analysis of the carotid sinus baroreflex system using a sum-of-sinusoidal input. Jpn J Physiol 42:15–34
6. Kawada T, Yanagiya Y, Uemura K, Miyamoto T, Zheng C, Li M, Sugimachi M, Sunagawa K (2002) Input-size dependence of the baroreflex neural arc transfer characteristics. Am J Physiol Heart Circ Physiol 284:H404–H415
7. Kawada T, Zheng C, Yanagiya Y, Uemura K, Miyamoto T, Inagaki M, Shishido T, Sugimachi M, Sunagawa K (2002) High-cut characteristics of the baroreflex neural arc preserve baroreflex gain against pulsatile pressure. Am J Physiol Heart Circ Physiol 282:H1149–H1156
8. Reid IA (1992) Interactions between ANG II, sympathetic nervous system, and baroreceptor reflexes in regulation of blood pressure. Am J Physiol Endocrinol Metab 262:E763–E778
9. Sanderford MG, Bishop VS (2000) Angiotensin II acutely attenuates range of arterial baroreflex control of renal sympathetic nerve activity. Am J Physiol Heart Circ Physiol 279:H1804–H1812
10. McMullan S, Goodchild AK, Pilowsky PM (2007) Circulating angiotensin II attenuates the sympathetic baroreflex by reducing the barosensitivity of medullary cardiovascular neurons in the rat. J Physiol 582:711–722
11. Kumagai K, Reid IA (1994) Angiotensin II exerts differential actions on renal nerve activity and heart rate. Hypertension 24:451–456
12. Tan PS, Killinger S, Horiuchi J, Dampney RA (2007) Baroreceptor reflex modulation by circulating angiotensin II is mediated by AT₁ receptors in the nucleus tractus solitarius. Am J Physiol Regul Integr Comp Physiol 293:R2267–R2278
13. Zucker IH (2006) Novel mechanisms of sympathetic regulation in chronic heart failure. Hypertension 48:1005–1011
14. Shoukas AA, Callahan CA, Lash JM, Haase EB (1991) New technique to completely isolate carotid sinus baroreceptor regions in rats. Am J Physiol Heart Circ Physiol 260:H300–H303
15. Sato T, Kawada T, Miyano H, Shishido T, Inagaki M, Yoshimura R, Tatewaki T, Sugimachi M, Alexander J Jr, Sunagawa K (1999) New simple methods for isolating baroreceptor regions of carotid sinus and aortic depressor nerves in rats. Am J Physiol Heart Circ Physiol 276:H326–H332
16. Grant TL, McGrath JC (1988) Interactions between angiotensin II, sympathetic nerve-mediated pressor response and cyclo-oxygenase products in the pithed rat. Br J Pharmacol 95:1220–1228
17. Haywood JR, Fink GD, Buggy J, Phillips MI, Brody MJ (1980) The area postrema plays no role in the pressor action of angiotensin in the rat. Am J Physiol Heart Circ Physiol 239:H108–H113
18. Kent BB, Drane JW, Blumenstein B, Manning JW (1972) A mathematical model to assess changes in the baroreceptor reflex. Cardiology 57:295–310
19. Glantz SA (2002) Primer of biostatistics, 5th edn. McGraw-Hill, New York
20. Mohrman DE, Heller LJ (2006) Cardiovascular physiology, 6th edn. McGraw Hill, New York, pp 172–177
21. Sato T, Kawada T, Inagaki M, Shishido T, Takaki H, Sugimachi M, Sunagawa K (1999) New analytic framework for